

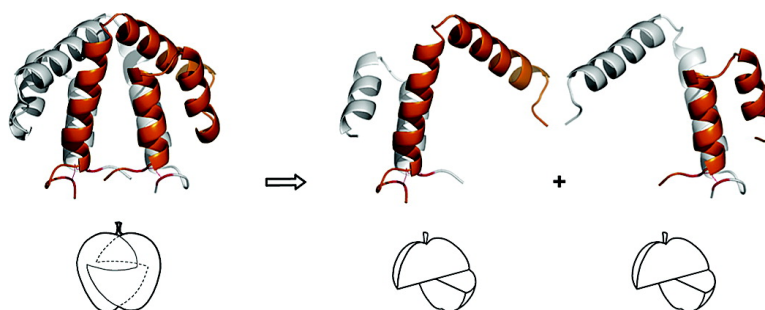
Article

Coupe du Roi Bisection of Proteins. Spontaneous Tetramerization of Two Peptides That Span the Sequence of the Rabbit Uteroglobulin Monomer

Ernesto Nicols, Cristina Ferrer, Lorena Taboada, and Ernest Giralt

J. Am. Chem. Soc., **2005**, 127 (50), 17719-17733 • DOI: 10.1021/ja0539793 • Publication Date (Web): 19 November 2005

Downloaded from <http://pubs.acs.org> on March 25, 2009



More About This Article

Additional resources and features associated with this article are available within the HTML version:

- Supporting Information
- Links to the 1 articles that cite this article, as of the time of this article download
- Access to high resolution figures
- Links to articles and content related to this article
- Copyright permission to reproduce figures and/or text from this article

[View the Full Text HTML](#)

Coupe du Roi Bisection of Proteins. Spontaneous Tetramerization of Two Peptides That Span the Sequence of the Rabbit Uteroglobulin Monomer

Ernesto Nicolás,^{*,†} Cristina Ferrer,[‡] Lorena Taboada,[§] and Ernest Giralt^{*,†,‡}

Contribution from the Department of Organic Chemistry, Martí i Franquès 1, and the Institut de Recerca en Biomedicina (Parc Científic de Barcelona), Josep Samitier 1–5, Universitat de Barcelona, Barcelona 08028, Spain

Received June 16, 2005; E-mail: enicolas@ub.edu

Abstract: The study of dividing objects into isometric segments has yielded novel approaches to the synthesis of high-symmetry organic compounds. Reported herein is the first application of this concept to a protein, rabbit uteroglobulin (UG). Bisection of UG into two identical homochiral segments led to the design of the heterodimeric 70mer peptide $\alpha(1,2)$ -S-S- $\alpha(3,4)$ that spans the sequence of the native UG monomer. The ability of this compound to form a globular 140mer tetramer consisting of two noncovalently bound heterodimers was assessed by ultracentrifugation at sedimentation equilibrium and by fluorescent spectroscopy. On the other hand, the monomeric peptides $\alpha(1,2)$ -SH and $\alpha(3,4)$ -SH were shown to selectively form the $\alpha(1,2)$ -S-S- $\alpha(3,4)$ heterodimer via spontaneous air oxidation in phosphate buffer at neutral pH.

Introduction

The problem of dividing finite geometric objects into isometric¹ segments has fascinated structural and synthetic chemists for decades. In a seminal paper from 1983, Mislow and colleagues² analyzed the intriguing way of cutting an apple known as “la coupe du roi”. Figure 1 illustrates how a pair of homochiral segments can be obtained from an achiral object (in this case, an apple) by first making two vertical half-cuts, one from the top to the equator and the other from the bottom to the equator, followed by two nonadjacent horizontal cuts. Although this concept has been applied to the retrosynthetic analysis of highly symmetric organic compounds such as fullerene C(60)³ or cyclic diketones⁴ as well as to helical organometallic compounds,⁵ to the best of our knowledge it has never before been applied to proteins.

Rabbit uteroglobulin (UG)⁶ is a steroid-inducible protein that belongs to the recently designated family of secretoglobins,⁷ small, evolutionarily conserved, multifunctional homodimeric secretory proteins found in mammals. They are produced by several mucosal epithelia and other organs of epithelial bronchoalveolar lavage fluid, serum, and urine.⁸

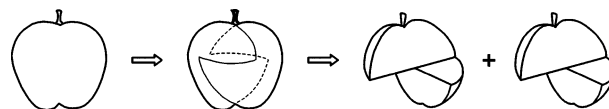


Figure 1. La coupe du roi. The apple yields a pair of isometric homochiral segments.

Despite more than three decades of research since the discovery of UG as the first known secretoglobulin,⁹ the primary physiological function of this family of proteins remains unknown. Nevertheless, a number of properties and functions of these proteins have been described.^{6b,10} Thus, it is believed that UG plays important immunosuppressive and anti-inflammatory roles by regulating immune reactions in epithelia of all organs that communicate with the external environment.¹¹ In

[†] Department of Organic Chemistry.

[‡] Parc Científic de Barcelona, Spain.

[§] Infar S.A., Barcelona, Spain.

[§] Lilly España S.A., Madrid, Spain.

- (1) In the context of chemistry, two molecules are considered isometric if their labeled graphs are the same, i.e., if the atoms and their connectivity (bonds) are the same. See refs 2 and 3, and references therein.
- (2) Anet, F. A. L.; Miura, S. S.; Siegel, J.; Mislow, K. *J. Am. Chem. Soc.* **1983**, *105*, 1419–1426.
- (3) Geneste, F.; Moradpour, A.; Dive, G.; Peeters, D.; Malthete, J.; Sadoc, J.-F. *J. Org. Chem.* **2002**, *67*, 605–607.
- (4) Cinquini, M.; Cozzi, F.; Sannicò, F.; Sironi, A. *J. Am. Chem. Soc.* **1988**, *110*, 4363–4364.
- (5) Glaser, R. *Chirality* **1993**, *5*, 272–276.

- (6) (a) Mukherjee, A. B.; Chilton, B. S., Eds. *The Uteroglobulin/Clara Cell Protein Family*; The New York Academy of Sciences: New York, 2000; Vol. 923, p 358. (b) Miele, L.; Cordella-Miele, E.; Mantile, G.; Peri, A.; Mukherjee, A. B. *J. Endocrinol. Invest.* **1994**, *17*, 679–692. (c) Mukherjee, A. B.; Kundu, G. C.; Mantile-Selvaggi, G.; Yuan, C. J.; Mandal, A. K.; Chattopadhyay, S.; Zheng, F.; Pattabiraman, N.; Zhang, Z. *Cell. Mol. Life Sci.* **1999**, *55*, 771–787.
- (7) Klug, J.; Beier, H. M.; Bernard, A.; Chilton, B. S.; Fleming, T. P.; Lehrer, R. I.; Miele, L.; Pattabiraman, N.; Singh, G. *Ann. N.Y. Acad. Sci.* **2000**, *923*, 348–354.
- (8) (a) Halatek, T.; Hermans, C.; Broeckeaert, F.; Wattiez, R.; Wiedig, M.; Toubeau, G.; Falmagne, P.; Bernard, A. *Eur. Respir. J.* **1998**, *11*, 726–733. (b) Aoki, A.; Pasolli, H. A.; Raida, M.; Meyer, M.; Schulz-Knappe, P.; Mostafavi, H.; Schepky, A. G.; Znotka, R.; Elia, J.; Hock, D.; Beier, H. M.; Forssmann, W. G. *Mol. Hum. Reprod.* **1996**, *2*, 489–497. (c) Bernard, A.; Roels, H.; Lauwerys, R.; Witters, R.; Gielens, C.; Soumillion, A.; Van Damme, J.; De Ley, M. *Clin. Chim. Acta* **1992**, *207*, 239–249. (d) Kikukawa, T.; Mukherjee, A. B. *Mol. Cell. Endocrinol.* **1989**, *62*, 177–187. (e) Shijubo, N.; Kawabata, I.; Sato, N.; Itoh, Y. *Curr. Pharm. Des.* **2003**, *9*, 1139–1149. (f) Jackson, P. J.; Turner, R.; Keen, J. N.; Brooksbank, R. A.; Cooper, E. H. *J. Chromatogr.* **1988**, *452*, 359–367.
- (9) (a) Beier, H. M. *Biochim. Biophys. Acta* **1968**, *160*, 289–291. (b) Krishnan, R. S.; Daniel, J. C., Jr. *Science* **1967**, *158*, 490–492.
- (10) (a) Miele, L.; Cordella-Miele, E.; Mukherjee, A. B. *Endocr. Rev.* **1987**, *8*, 474–490. (b) Singh, G.; Katyal, S. L. *Ann. N.Y. Acad. Sci.* **2000**, *923*, 43–58.

this sense, UG is a potent inhibitor of secretory and cytosolic phospholipase A2, a proinflammatory enzyme,^{10a,12} and modulates levels of γ -interferon, a potent proinflammatory cytokine that induces a wide range of immunological activities.¹³ UG also prevents abnormal deposition of fibronectin, which leads to renal inflammatory diseases such as fibronectin deposit glomerulopathy.^{6c,14} On the other hand, recent studies have revealed that UG can act as a tumor suppressor via inhibition of cell chemoinvasion.^{15,16} How these functions are exerted by the protein has not been established, although their mediation by cell surface membrane proteins that act as receptors has been imputed.^{16,17} UG can also function as an inhibitor and/or a carrier protein by complexing with small molecules such as endogenous substrates (e.g., phospholipids,¹⁸ progesterone,¹⁹ retinol,²⁰ or calcium ion²¹) and xenobiotics (e.g., polychlorobiphenyls²² and naphthalene²³). The physiological functions related to this property remain an enigma, but it has been speculated that UG may prevent the degradation of the protein-bound substrate, thereby prolonging its biological activity. UG could also serve as a carrier protein for the removal of toxic agents to prevent further pathogenicity toward an organism, especially in the lungs, where UG is the main product secreted by Clara cells, the bronchiolar cell type most reactive to toxic xenobiotics.²⁴

The functional diversity of UG-like proteins stems from their relevant molecular recognition properties, which in turn result from a shared, particular tertiary structure. UG consists of two

identical polypeptide chains 70 amino acids in length (Figure 2a). X-ray²⁵ and NMR²⁶ studies reveal that both monomers are arranged in an antiparallel fashion that forms a compact globular structure with a pseudo- C_2 axis in which each monomer has four α -helices (α_1 , α_2 , α_3 , and α_4) generally separated by β bends (Figure 2b). These helices are packed in a boomerang-shaped motif in which α_1 , α_3 , and α_4 form a dimeric structure displaying a large oblong internal hydrophobic cavity of 440 Å³, whereas the interfacing helices α_1 and α_4' (the latter belonging to the other subunit) form a canonical "square bundle" together with α_4 and α_1' .²⁷ The internal cavity can accommodate small- to medium-sized hydrophobic ligands, but access to it is restricted by the intermolecular disulfide bridges that hold the two monomers together.

It is interesting to note that, although the various species of the UG family exhibit only 50–60% homology in the amino acid sequences of their monomers,²⁸ structural studies reveal that these proteins have similar 3-D folding and share the same crucial residues responsible for their biological functions. In this sense, the residues that line the hydrophobic pocket are highly conserved, and the substitutions in those positions are almost invariably conservative. Furthermore, the residues Lys43 and Asp46, which are involved in phospholipase A2 inhibition,²⁹ are also present in most of the proteins isolated to date. In fact, UG and its human counterpart are the most widely studied secretoglobins and have been experimentally determined to be both structurally³⁰ and functionally^{12c} indistinguishable.

As shown in Figure 2b, the 140mer UG molecule can be dissected into two identical homochiral 70mers, HS- $\alpha(1,2,3,4)$ -SH, by cleavage of the two S–S disulfide bonds. This process corresponds to the reduction of UG to UG-[red] that is well documented in the literature and that preserves the globular structure as well as most of the molecular recognition properties of UG (see below). In this sense, a variety of monomeric proteins have been divided into two fragments by chemical, proteolytic, or genetic means, to create interchain-packed, active functional proteins.³¹ This approach, which has been termed "protein fragment complementation", has been used to examine theories of protein evolution,^{32a} protein folding,^{32b,c} macromolecular assembly,^{32d} and structure–function relationships,^{32e} and for mapping contacts in membrane-embedded proteins.^{32f} Figure 2c shows an unprecedented way of dissecting UG, inspired by "la coupe du roi", that leads to two identical disulfide 70mers, $\alpha(1,2)$ -S-S- $\alpha(3,4)$. The present paper describes the conforma-

- (11) (a) Mukherjee, A. B.; Cordella-Miele, E.; Kikukawa, T.; Miele, L. *Adv. Exp. Med. Biol.* **1988**, *231*, 135–152. (b) Mukherjee, A. B.; Ulane, R. E.; Agrawal, A. K. *Am. J. Reprod. Immunol.* **1982**, *2*, 135–141. (c) Mukherjee, D. C.; Agrawal, A. K.; Manjunath, R.; Mukherjee, A. B. *Science* **1983**, *219*, 989–991.
- (12) (a) Lesur, O.; Bernard, A.; Arsalane, K.; Lauwerys, R.; Begin, R.; Cantin, A.; Lane, D. *Am. J. Respir. Crit. Care Med.* **1995**, *152*, 290–297. (b) Levin, S. W.; Butler, J. D.; Schumacher, U. K.; Wightman, P. D.; Mukherjee, A. B. *Life Sci.* **1986**, *38*, 1813–1819. (c) Mantile, G.; Miele, L.; Cordella-Miele, E.; Singh, G.; Katyal, S. L.; Mukherjee, A. B. *J. Biol. Chem.* **1993**, *268*, 20343–20351. (d) Miele, L.; Cordella-Miele, E.; Mukherjee, A. B. *J. Biol. Chem.* **1990**, *265*, 6427–6435.
- (13) (a) Chang, A.; Ramsay, P.; Zhao, B.; Park, M.; Magdaleno, S.; Reardon, M. J.; Welty, S.; Demayo, F. *J. Ann. N.Y. Acad. Sci.* **2000**, *923*, 181–192. (b) Dierynck, I.; Bernard, A.; Roels, H.; De Ley, M. *Am. J. Respir. Cell Mol. Biol.* **1995**, *12*, 205–210. (c) Ramsay, P. L.; Luo, Z.; Magdaleno, S. M.; Whitbourne, S. K.; Cao, X.; Park, M. S.; Welty, S. E.; Yu-Lee, L. Y.; DeMayo, F. *J. Am. J. Physiol.* **2003**, *284*, L108–L118.
- (14) (a) Zhang, Z.; Kundu, G. C.; Yuan, C. J.; Ward, J. M.; Lee, E. J.; DeMayo, F.; Westphal, H.; Mukherjee, A. B. *Science* **1997**, *276*, 1408–1412. (b) Zheng, F.; Kundu, G. C.; Zhang, Z.; Ward, J.; DeMayo, F.; Mukherjee, A. B. *Nat. Med.* **1999**, *5*, 1018–1025.
- (15) (a) Szabo, E.; Goheer, A.; Witschi, H.; Linnoila, R. I. *Cell Growth Differ.* **1998**, *9*, 475–485. (b) Leyton, J.; Manyak, M. J.; Mukherjee, A. B.; Miele, L.; Mantile, G.; Patierno, S. R. *Cancer Res.* **1994**, *54*, 3696–3699.
- (16) (a) Kundu, G. C.; Mandal, A. K.; Zhang, Z.; Mantile-Selvaggi, G.; Mukherjee, A. B. *J. Biol. Chem.* **1998**, *273*, 22819–22824. (b) Kundu, G. C.; Mantile, G.; Miele, L.; Cordella-Miele, E.; Mukherjee, A. B. *Proc. Natl. Acad. Sci. U.S.A.* **1996**, *93*, 2915–2919. (c) Zhang, Z.; Kundu, G. C.; Panda, D.; Mandal, A. K.; Mantile-Selvaggi, G.; Peri, A.; Yuan, C. J.; Mukherjee, A. B. *Proc. Natl. Acad. Sci. U.S.A.* **1999**, *96*, 3963–3968.
- (17) Diaz Gonzalez, K.; Nieto, A. *FEBS Lett.* **1995**, *361*, 255–258.
- (18) Umland, T. C.; Swaminathan, S.; Singh, G.; Warty, V.; Furey, W.; Pletcher, J.; Sax, M. *Nat. Struct. Biol.* **1994**, *1*, 538–545.
- (19) (a) Beato, M. *J. Steroid Biochem.* **1976**, *7*, 327–334. (b) Singh, G.; Katyal, S. L.; Brown, W. E.; Kennedy, A. L. *Exp. Lung Res.* **1993**, *19*, 67–75.
- (20) Lopez de Haro, M. S.; Perez Martinez, M.; Garcia, C.; Nieto, A. *FEBS Lett.* **1994**, *349*, 249–251.
- (21) Barnes, H. J.; Nordlund-Moller, L.; Nord, M.; Gustafsson, J.; Lund, J.; Gillner, M. *J. Mol. Biol.* **1996**, *256*, 392–404.
- (22) (a) Andersson, O.; Nordlund-Moller, L.; Barnes, H. J.; Lund, J. *J. Biol. Chem.* **1994**, *269*, 19081–19087. (b) Andersson, O.; Nordlund-Moller, L.; Bronnegard, M.; Sirzea, F.; Ripe, E.; Lund, J. *Am. J. Respir. Cell Mol. Biol.* **1991**, *5*, 6–12. (c) Gillner, M.; Lund, J.; Cambillau, C.; Alexandersson, M.; Hurtig, U.; Bergman, A.; Klasson-Wehler, E.; Gustafsson, J. A. *J. Steroid Biochem.* **1988**, *31*, 27–33. (d) Stripp, B. R.; Lund, J.; Mango, G. W.; Doyen, K. C.; Johnston, C.; Hultenby, K.; Nord, M.; Whitsett, J. A. *Am. J. Physiol.* **1996**, *271*, L656–L664.
- (23) Stripp, B. R.; Maxson, K.; Mera, R.; Singh, G. *Am. J. Physiol.* **1995**, *269*, L791–L799.
- (24) Elia, J.; Aoki, A.; Maldonado Cristina, A. *Histochem. Cell Biol.* **2003**, *120*, 33–39.

- (25) (a) Bally, R.; Delettre, J. *J. Mol. Biol.* **1989**, *206*, 153–170. (b) Mornon, J. P.; Fridlansky, F.; Bally, R.; Milgrom, E. *J. Mol. Biol.* **1980**, *137*, 415–429.
- (26) Winkelmann, R.; Geschwindner, S.; Haun, M.; Ruterjans, H. *Eur. J. Biochem.* **1998**, *258*, 521–532.
- (27) Lin, S. L.; Tsai, C. J.; Nussinov, R. *J. Mol. Biol.* **1995**, *248*, 151–161.
- (28) Ni, J.; Kalfif-Suske, M.; Gentz, R.; Schageman, J.; Beato, M.; Klug, J. *Ann. N.Y. Acad. Sci.* **2000**, *923*, 25–42.
- (29) Chowdhury, B.; Mantile-Selvaggi, G.; Miele, L.; Cordella-Miele, E.; Zhang, Z.; Mukherjee, A. B. *Biochem. Biophys. Res. Commun.* **2002**, *295*, 877–883.
- (30) Callebaut, I.; Poupon, A.; Bally, R.; Demaret, J.-P.; Housset, D.; Delettre, J.; Hossenlopp, P.; Mornon, J.-P. In *The Uteroglobin/Clara Cell Protein Family*; Mukherjee, A. B., Chilton, B. S., Eds.; The New York Academy of Sciences: New York, 2000; Vol. 923, pp 90–112.
- (31) (a) Ullmann, A.; Jacob, F.; Monod, J. *J. Mol. Biol.* **1967**, *24*, 339–343. (b) Kato, I.; Anfinsen, C. B. *J. Biol. Chem.* **1969**, *244*, 1004–1007.
- (32) (a) Bertolaet, B. L.; Knowles, J. R. *Biochemistry* **1995**, *34*, 5736–5743. (b) Ladurner, A. G.; Itzhaki, L. S.; Gray, G. P.; Fersht, A. R. *J. Mol. Biol.* **1997**, *273*, 317–329. (c) de Prat Gay, G.; Ruiz-Sanz, J.; Fersht, A. R. *Biochemistry* **1994**, *33*, 7957–7963. (d) Tasayco, M. L.; Carey, J. *Science* **1992**, *255*, 594–597. (e) Shiba, K.; Schimmel, P. *Proc. Natl. Acad. Sci. U.S.A.* **1992**, *89*, 1880–1884. (f) Yu, H.; Kono, M.; McKee, T. D.; Oprian, D. D. *Biochemistry* **1995**, *34*, 14963–14969.

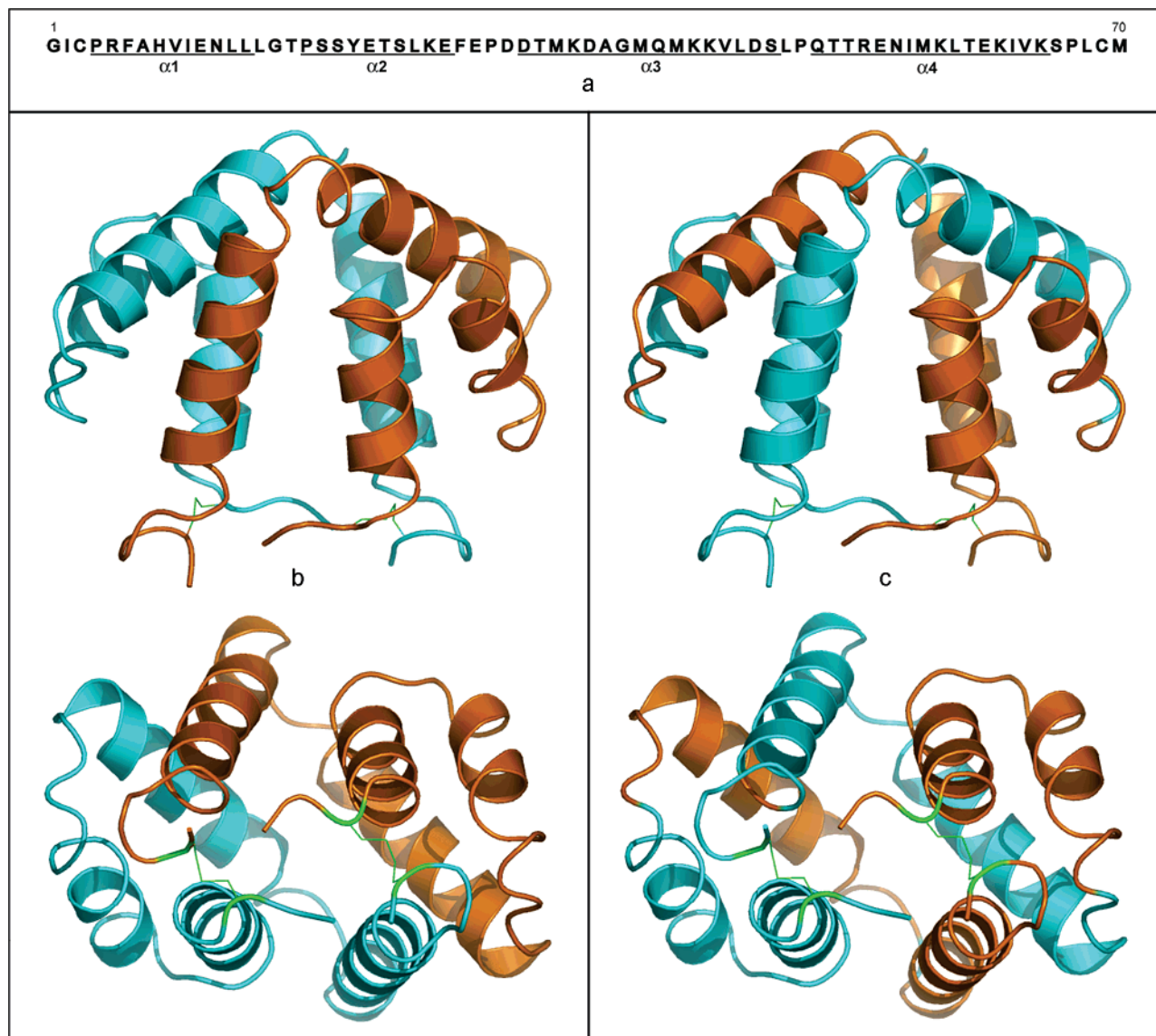


Figure 2. Tertiary structure of rabbit UG from X-ray data of crystal $P2_1$ (see ref 25a). (a) The sequence of the monomer. (b) Two identical halves, HS- $\alpha(1,2,3,4)$ -SH, can be generated by dissecting the molecule via reduction of the disulfide bonds. (c) Alternatively, two identical halves, $\alpha(1,2)$ -S-S- $\alpha(3,4)$, can result from the “virtual” hydrolysis of two peptide bonds connecting helices 2 and 3.

tional and self-assembly properties of the molecule generated by this new disconnection mode.

Results and Discussion

Design Principles. The intriguing molecular recognition properties of UG, its numerous biological functions, and the growing interest in its application in the design of potential diagnostic and therapeutic agents for pulmonary, renal, and oncological diseases^{8e,33} prompted us to devote a line of research to study this molecule from synthetic and structural points of view. The availability of a plasmid for the expression of rabbit UG drew our attention to this particular UG form.^{12d,34} The study of the conformational and self-assembly behavior of UG fragments was thus undertaken. In looking at how both UG monomers are packed together to form the globular 3-D structure, it seems obvious that the helix motif plays an

important role in stabilizing the structure through interchain helical interactions, a feature that is probably required for head-to-tail self-assembly of the monomer. Experiments employing fragments that span helical regions of rabbit UG monomer were thus designed and executed to find evidence of helix-to-helix recognition. There is literature precedent for the use of peptides corresponding to fragments of this polypeptide in structural studies.³⁵ These experiments have focused primarily on peptides containing $\alpha 3$, owing to its implication in the phospholipase A2 inhibitory and anti-inflammatory activities of the protein.^{29,36} In the case at hand, the square bundle motif was considered an attractive starting point because interactions between N-terminal helix $\alpha 1(1')$ and C-terminal helix $\alpha 4(4')$ could be revealed using suitable peptide models. Thus, the Cys-containing peptides corresponding to sequences 1–14 ($\alpha 1$ -SH) and 48–70 ($\alpha 4$ -SH) of the monomer of rabbit UG were

(33) Pilon, A. L. *Ann. N.Y. Acad. Sci.* **2000**, *923*, 280–299.

(34) Mantile, G.; Fuchs, C.; Cordella-Miele, E.; Peri, A.; Mukherjee, A. B.; Miele, L. *Biotechnol. Prog.* **2000**, *16*, 17–25.

(35) (a) Improta, S.; Pastore, A.; Mammi, S.; Peggion, E. *Biopolymers* **1994**, *34*, 773–782. (b) Mammi, S.; Foffani, M. T.; Improta, S.; Tessari, M.; Schievano, E.; Peggion, E. *Biopolymers* **1992**, *32*, 341–346.

(36) Moreno, J. J. *Ann. N.Y. Acad. Sci.* **2000**, *923*, 147–153.

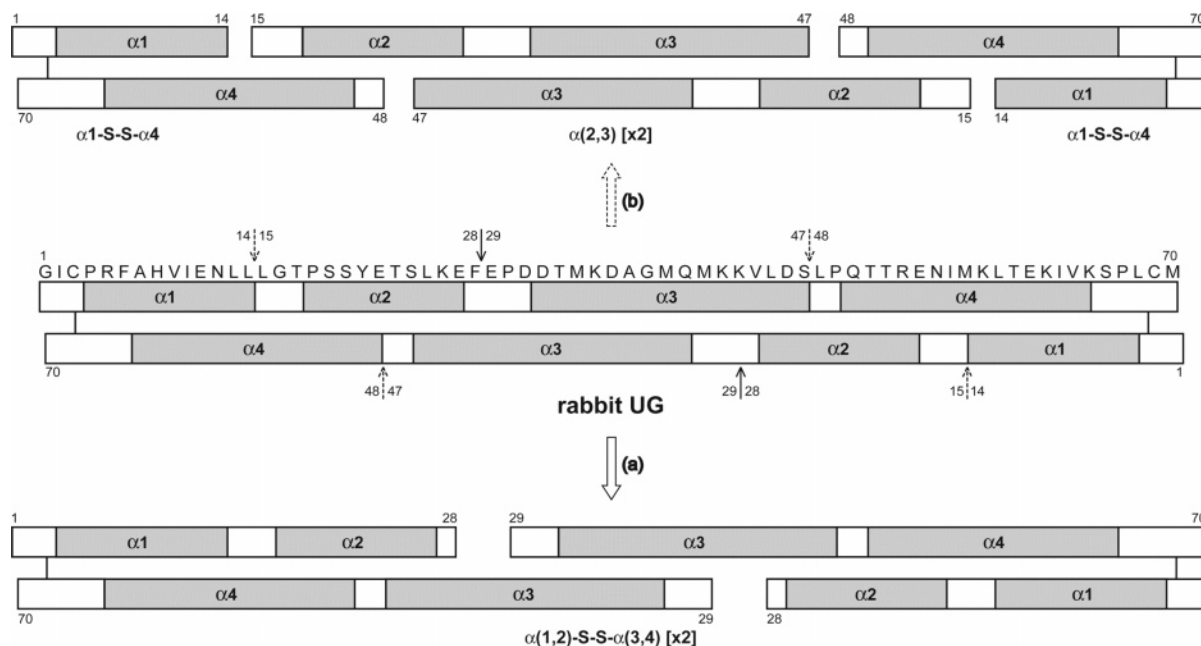


Figure 3. Schematic representation of the covalent dimeric rabbit UG and the nicked proteins studied in this work: (a) four-helix fragment $\alpha(1,2)$ -S-S- $\alpha(3,4)$; (b) two-helix fragments $\alpha 1$ -S-S- $\alpha 4$ and $\alpha(2,3)$.

synthesized in the solid phase following standard protocols, and their propensity to spontaneously form disulfide bridges was studied. Aqueous CD studies revealed negative absorption for both peptides at 200 nm, indicative of a largely random coil conformation. However, titration with 2,2,2-trifluoroethanol (TFE) resulted in an increase in negative ellipticity at 208 and 222 nm and increasingly positive ellipticity at 194 nm, consistent with a structural transition to an α -helix in the presence of the organic cosolvent.³⁷ Dimerization (homo or hetero) did not occur when $\alpha 1$ -SH and $\alpha 4$ -SH were combined in water under air oxidation conditions (75 μ M concentration of each peptide, 5 mM phosphate buffer at pH 7.1, room temperature), whereas the heterodimer $\alpha 1$ -S-S- $\alpha 4$ was the only product detected when TFE was added to the reaction mixture (30%).³⁸ The high tendency to heterodimerize in the presence of TFE suggests that specific helicoidal interchain interactions between $\alpha 1$ -SH and $\alpha 4$ -SH must be responsible for the head-to-tail orientation of these peptides suitable for the generation of $\alpha 1$ -S-S- $\alpha 4$ containing the native disulfide bridge. TFE contributes to formation of the heterodimer via helix promotion in the monomers because they are randomly coiled in the absence of structuring agent. On the other hand, the disulfide bridge does not contribute to secondary structure stabilization in $\alpha 1$ -S-S- $\alpha 4$ because it is unable to achieve any defined structure in water. This result can be understood in the context of the absence of helices $\alpha 2$ and $\alpha 3$ in $\alpha 1$ -S-S- $\alpha 4$ and, therefore, the lack of interactions in which such helices are involved in the native protein, where they form two α -hairpins that wrap onto helices $\alpha 1$ and $\alpha 4$ as shown in Figure 2.

The preliminary results obtained with the peptides $\alpha 1$ -SH and $\alpha 4$ -SH using the disulfide trapping approach to reveal helix-to-helix interactions inspired similar studies for peptides that contain multiple helices. In this sense, the use of peptides corresponding to N-terminal and C-terminal sequences of the

protein monomer that contain two helices was appealing when the 3-D structure of the native molecule was taken into account. Thus, the two monomers are assembled head-to-tail to form a globular structure with a C_2 axis that can be split into two identical units of the disulfide containing heterodimer $\alpha(1,2)$ -S-S- $\alpha(3,4)$ by the “coupe du roi” approach (Figure 3a).² In other words, the resulting peptide spans the whole sequence of the native monomer with a different topology. Hence the structural behavior of the peptides corresponding to the complementary sequences 1–28 ($\alpha(1,2)$ -SH) and 29–70 ($\alpha(3,4)$ -SH), as well as their propensity to form $\alpha(1,2)$ -S-S- $\alpha(3,4)$, was studied. We envisioned that spontaneous self-assembly of this peptide would yield a tetramer formed by two noncovalently bound molecules of heterodimer ($[\alpha(1,2)$ -S-S- $\alpha(3,4)]_2$), structurally similar to UG and, consequently, having analogous molecular recognition properties.

The self-assembly hypothesis can be extended to other two-helix-containing peptides such as $\alpha 1$ -S-S- $\alpha 4$ and the complementary peptide spanning the sequence 15–47 of the native monomer ($\alpha(2,3)$, Figure 3b), although two cuts of the UG monomer would be necessary in this case. The possibility that $\alpha 1$ -S-S- $\alpha 4$ and $\alpha(2,3)$ could interact to promote 3-D structure by fragment complementation was also explored to compare the results with those of the “coupe du roi” approach.

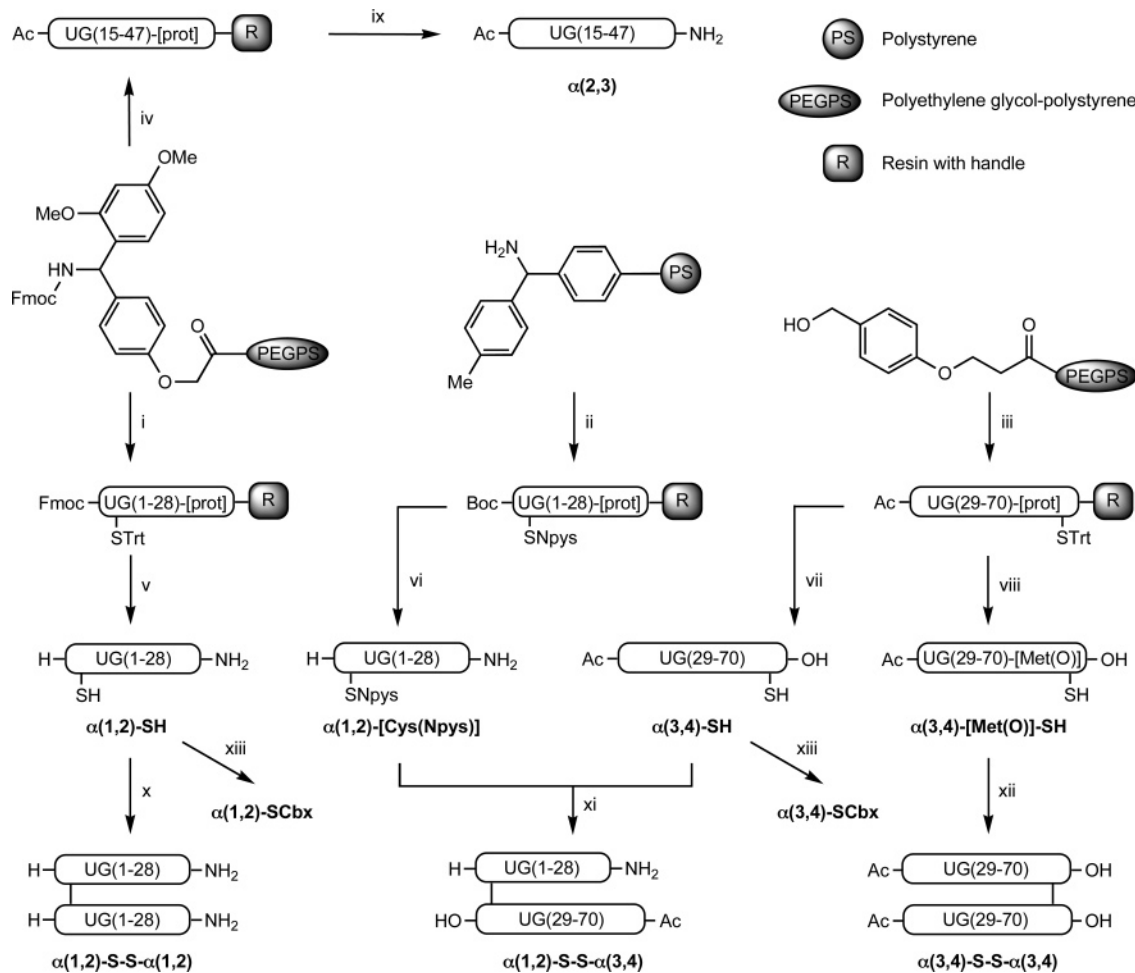
Peptide Synthesis. All peptides for this work were synthesized in the solid phase³⁹ via *tert*-butoxycarbonyl (Boc) or 9-fluorenylmethoxycarbonyl (Fmoc) strategies,⁴⁰ except for the *S*-carboxymethylated analogues of wild-type $\alpha(1,2)$ -SH and $\alpha(3,4)$ -SH ($\alpha(1,2)$ -SCbx and $\alpha(3,4)$ -SCbx), which were prepared in solution (Scheme 1). Amino acid side chains were protected with the groups traditionally used for these chemistries, and the Met residue was also protected as its corresponding sulfoxide. Peptides were acetylated at the N-terminal and/or carboxyami-

(37) Nicolas, E.; Bacardit, J.; Ferrer, T.; Giralt, E. *Lett. Pept. Sci.* **1996**, *2*, 353–362.

(38) Ferrer, T.; Nicolas, E.; Giralt, E. *Lett. Pept. Sci.* **1999**, *6*, 165–172.

(39) Merrifield, R. B. *J. Am. Chem. Soc.* **1963**, *85*, 2149–2154.

(40) Lloyd-Williams, P.; Albericio, F.; Giralt, E. *Chemical Approaches to the Synthesis of Peptides and Proteins*; CRC Press: Boca Raton, 1997; p 297.

Scheme 1. Synthetic Route for the Peptides Used in This Study^a

^a (i) 28 cycles solid-phase peptide synthesis (SPPS). (ii) (a) Boc-Phe-OH, DCC; (b) 27 cycles SPPS. (iii) (a) Fmoc-Met(O)-OH, DIPCDI, DMAP; (b) 41 cycles SPPS; (c) Ac₂O, DIEA. (iv) (a) 32 cycles SPPS; (b) Ac₂O, DIEA. (v) TFA/H₂O/TES (90:5:5). (vi) High HF. (vii) Low–high HF. (viii) TFA/anisole/EDT/thioanisole (90:2:3:5). (ix) (a) TFA/anisole/EDT/thioanisole (90:2:3:5); (b) Bu₄NBr/TFA. (x) O₂, pH 8. (xi) Aqueous AcOH, pH 4. (xii) NH₄I, Me₂S, TFA. (xiii) ICH₂CONH₂, pH 8.2.

dated at the C-terminal in order to mimic a peptide bond in the natural sequence.

Peptides $\alpha(1,2)$ -SH and $\alpha(2,3)$ were manually assembled using Fmoc chemistry on a poly(ethylene glycol)–polystyrene resin (PEG-PS) resin that was previously functionalized with the modified Rink amide linker in order to obtain the peptide as a C-terminal carboxamide.⁴¹ The former was constructed via the symmetrical anhydride formed using 1,3-diisopropylcarbodiimide (DIPCDI), or via the active ester resulting from reaction with DIPCDI and *N*-hydroxybenzotriazole (HOBt) (Arg5, Asn12, Glu11, Glu22, Glu27). Coupling of Thr17 to Pro18 proved to be difficult, and *O*-(7-azabenzotriazol-1-yl)-*N,N,N',N'*-tetramethyluronium hexafluorophosphate (HATU) was ultimately required for amino acid activation. In the case of $\alpha(2,3)$, amino acids were coupled with DIPCDI/HOBt (sequence 38–47) and *O*-(benzotriazol-1-yl)-*N,N,N',N'*-tetramethyluronium tetrafluoroborate (TBTU)/*N,N*-diisopropylethylamine (DIEA) (sequence 15–37). Peptide $\alpha(1,2)$ -SH was cleaved from the resin and fully deprotected by treatment with trifluoroacetic acid (TFA) in the presence of water and triethylsilane (TES) as scavengers (TFA/H₂O/TES, 90:5:5). To obtain $\alpha(2,3)$, cleavage

from the resin and full deprotection was accomplished using reagent R (TFA/anisole/1,2-ethanedithiol (EDT)/thioanisole, 90:2:3:5)⁴² and subsequent treatment with a reducing agent to remove the sulfoxide moiety from protected Met residues. NH₄I,⁴³ TMSBr,⁴⁴ and Bu₄NBr or Bu₄NI⁴⁵ all proved to be efficient for this purpose. Peptides $\alpha(1,2)$ -SH (Figure 4a) and $\alpha(2,3)$ were obtained in 25% and 13% yields, respectively, after purification by reverse-phase chromatography (RP-MPLC) of the crudes that resulted from the acidolytic cleavage of the corresponding peptidyl resins.

Peptide $\alpha(3,4)$ -SH was prepared on a PEG-PS resin to which the handle 3-(4-hydroxymethylphenoxy)propionic acid (PAB) was anchored prior to automated synthesis of the peptide chain.⁴⁶ Met70 was linked to the hydroxyl function of the polymeric support using DIPCDI in the presence of catalytic *N,N*-dimethylaminopyridine (DMAP), whereas the remaining amino acids were attached to the resin via TBTU/DIEA activation.

(41) Breipohl, G.; Knolle, J.; Geiger, R. *Tetrahedron Lett.* **1987**, *28*, 5647–5650.

(42) Albericio, F.; Kneib-Cordonier, N.; Biancalana, S.; Gera, L.; Masada, R. I.; Hudson, D.; Barany, G. *J. Org. Chem.* **1990**, *55*, 3730–3743.

(43) Vilaseca, M.; Nicolas, E.; Capdevila, F.; Giralt, E. *Tetrahedron* **1998**, *54*, 15273–15286.

(44) Beck, W.; Jung, G. *Let. Pept. Sci.* **1994**, *1*, 31–37.

(45) Taboada, L.; Nicolas, E.; Giralt, E. *Tetrahedron Lett.* **2001**, *42*, 1891–1893.

(46) Albericio, F.; Barany, G. *Int. J. Pept. Protein Res.* **1985**, *26*, 92–97.

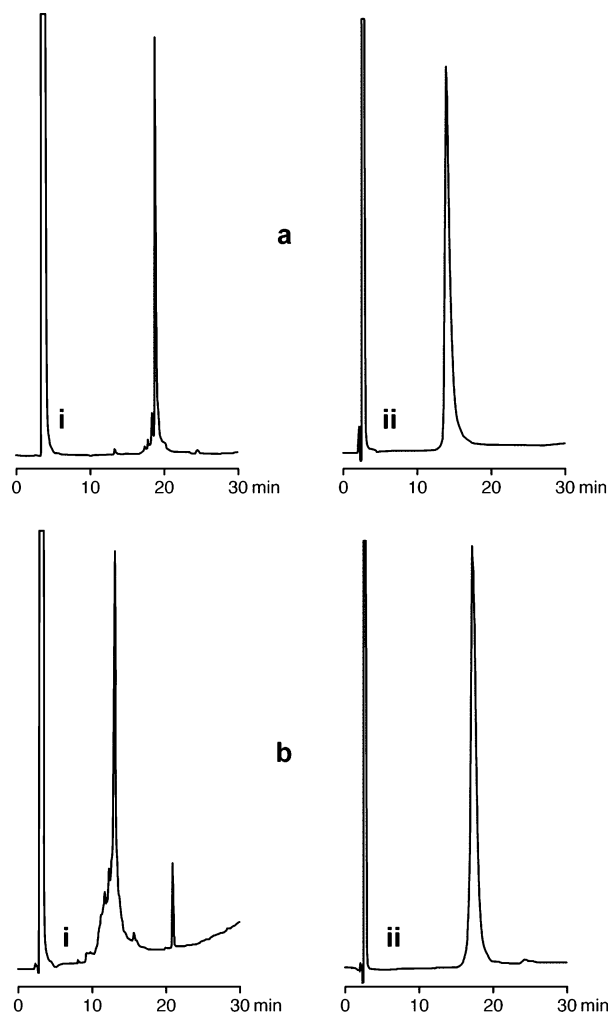


Figure 4. Analytical reverse-phase HPLC of $\alpha(1,2)$ -SH (a) and $\alpha(3,4)$ -SH (b), before (i) and after (ii) semipreparative purification. HPLC conditions: linear gradient from 10% to 100% B (a-i, b-i) and from 25% to 30% B (a-ii, b-ii); A, H₂O, 0.045% TFA and B, MeCN, 0.036% TFA; 1 mL/min, 220 nm.

The peptide was cleaved from the resin, fully deprotected with low–high HF,⁴⁷ and purified by RP-MPLC with a final yield of 15% (Figure 4b). Treatment of the same peptidyl resin with reagent R afforded the partially deprotected peptide $\alpha(3,4)$ -[Met(O)]-SH in 45% yield after RP-MPLC purification. The peptides $\alpha(1,2)$ -SCbx and $\alpha(3,4)$ -SCbx were obtained in solution from the corresponding Cys-unprotected peptides in 42% and 41% yields, respectively, by reaction with iodoacetamide at pH 8.2.⁴⁸

The three possible products resulting from spontaneous dimerization of $\alpha(1,2)$ -SH and $\alpha(3,4)$ -SH were also synthesized for the purpose of characterization. Disulfides were formed in solution using different protocols. Thus, air oxidation of $\alpha(1,2)$ -SH yielded the corresponding homodimer $\alpha(1,2)$ -S-S- $\alpha(1,2)$ in 60% yield, and deprotection of $\alpha(3,4)$ -[Met(O)]-SH with concomitant Cys oxidation using NH₄I/Me₂S/TFA yielded the homodimer $\alpha(3,4)$ -S-S- $\alpha(3,4)$ in 70% yield.⁴³ Heterodimer $\alpha(1,2)$ -S-S- $\alpha(3,4)$ was prepared from peptides 3-nitro-2-pyridine-sulfonyl-Cys-protected $\alpha(1,2)$ -[Cys(Npys)] and $\alpha(3,4)$ -SH through nucleophilic displacement of the Npys group by the thiol group

(30%).⁴⁹ The peptide $\alpha(1,2)$ -[Cys(Npys)] was synthesized automatically using Boc chemistry on a *p*-methylbenzhydrylamine resin (MBHA) resin to afford the peptide as a carboxamide.⁵⁰ Amino acid couplings were performed with *N,N*-dicyclohexylcarbodiimide (DCC) using the symmetric anhydride method, except in the cases of Asn and Arg, in which DCC/HOBt was used. Incorporation of Thr required activation with HATU. Side-chain deprotection and cleavage of the peptide from the resin were achieved with high-concentration HF.⁵¹ The peptide was obtained in 40% yield after RP-MPLC purification. The heterodimer $\alpha(1)$ -S-S- $\alpha(4)$ was obtained as previously reported.³⁸

Circular Dichroism. Beginning with the study of $\alpha(1,2)$ -S-S- $\alpha(3,4)$, the first goal was to determine if the model peptides $\alpha(1,2)$ -SH and $\alpha(3,4)$ -SH were able to achieve secondary structure in water in a way similar to what had been done with the heterodimer $\alpha(1)$ -S-S- $\alpha(4)$. As observed for peptides $\alpha(1)$ -SH and $\alpha(4)$ -SH, neither $\alpha(1,2)$ -SH nor $\alpha(3,4)$ -SH had helical properties under the conditions used (75 μ M peptide, phosphate buffer at pH 7.1, 5 °C), but a tendency to adopt α -helix structure with increasing quantities of TFE or 1,1,1,3,3,3-hexafluoro-2-propanol (HFIP) was shown. It should be mentioned that spontaneous homodimerization of $\alpha(1,2)$ -SH or $\alpha(3,4)$ -SH was not detected by reverse-phase HPLC during the CD experiments despite the presence of unprotected Cys residues. Interestingly, and unlike $\alpha(1)$ -S-S- $\alpha(4)$, the four-helix-containing heterodimer $\alpha(1,2)$ -S-S- $\alpha(3,4)$ showed a typical α -helix spectrum by CD in the absence of structuring agent. The percentage of helix, determined by measuring ellipticity at 222 nm under Yang parameters, was lower than that of recombinant rabbit UG molecule (38% and 63%, respectively), but the two spectra became very similar upon addition of TFE (30%), as shown in Figure 5a. On the other hand, $\alpha(1,2)$ -S-S- $\alpha(3,4)$ was more sensitive to thermal denaturation than the protein, as shown by monitoring the temperature dependence of the dichroic signal at 222 nm (Figure 5a, inset). Thus, the peptide proved to be stable in the range of 10–40 °C, and the decrease in helicity began to be appreciable above 40 °C, achieving a maximum value at 80 °C. However, unfolding of the recombinant rabbit UG molecule proceeded slowly along the same temperature range. Carlomagno et al.⁵² have also reported remarkable thermal stability for recombinant human UG, a protein for which the temperature of denaturation failed to reach a plateau even at 108 °C. The significant loss of helical content observed for $\alpha(1,2)$ -S-S- $\alpha(3,4)$ (ca. 50%), compared to that for the native protein (ca. 25%), can be attributed to the covalent nature of the two-disulfide-containing homodimer of the latter that contributes to the stabilization of the antiparallel assembly of the monomers. However, other contributions to this result cannot be ruled out, such as a non-native helix–helix interpacking or a decreased overall content of secondary structure in $\alpha(1,2)$ -S-S- $\alpha(3,4)$ at low temperature.

The high propensity of $\alpha(1,2)$ -S-S- $\alpha(3,4)$ to extensively adopt a helical secondary structure in water suggests that the molecule could form a globular structure. The fact that this peptide

(47) Tam, J. P.; Heath, W. F.; Merrifield, R. B. *J. Am. Chem. Soc.* **1983**, *105*, 6442–6455.

(48) Sanyal, G.; Marquis-Omer, D.; Waxman, L.; Mach, H.; Ryan, J. A.; O'Brien Gress, J.; Middaugh, C. R. *Biochim. Biophys. Acta* **1995**, *1249*, 100–108.

(49) Andreu, D.; Albericio, F.; Sole, N. A.; Munson, M. C.; Ferrer, M.; Barany, G. *Methods Mol. Biol.* **1994**, *35*, 91–169.

(50) Matsueda, G. R.; Stewart, J. M. *Peptides* **1981**, *2*, 45–50.

(51) Tam, J. P.; Merrifield, R. B. In *Peptides*; Udenfriend, S., Meienhofer, J., Eds.; Academic Press: New York, 1987; Vol. 9, pp 185–248.

(52) Carlomagno, T.; Mantile, G.; Bazzo, R.; Miele, L.; Paolillo, L.; Mukherjee, A. B.; Barbato, G. *J. Biomol. NMR* **1997**, *9*, 35–46.

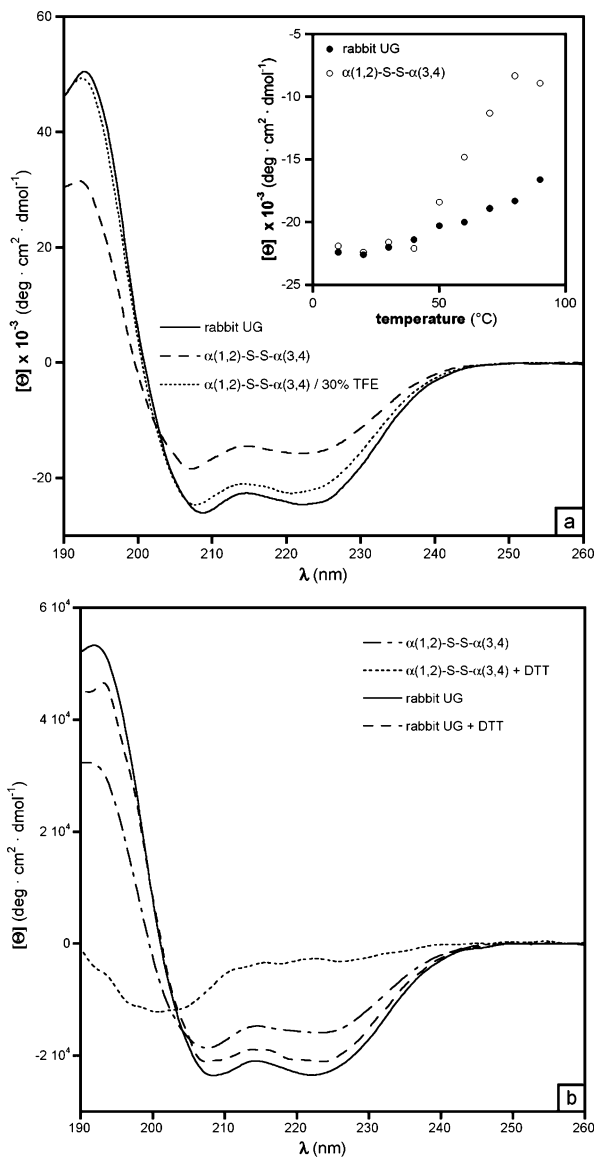


Figure 5. Far-UV CD analysis of rabbit UG and $\alpha(1,2)$ -S-S- $\alpha(3,4)$: spectra of (a) the disulfide containing wild-type protein ($5 \mu\text{M}$) and the peptide ($25 \mu\text{M}$), and (b) the corresponding reduced forms. Inset: Unfolding of the protein ($5 \mu\text{M}$) and the peptide ($20 \mu\text{M}$) measured by the effect of temperature on the mean residue ellipticity $[\Theta]$ at 220 nm. Measurements were carried out in 5 mM phosphate buffer (pH 7.1) and spectra were recorded at 25°C . Disulfide bonds were reduced with DTT (2 mM) at 37°C for 2 h.

constitutes the full-length sequence of the monomer of rabbit UG could explain the stabilization of such globular structure through intermolecular hydrophobic interactions via formation of the tetramer $[\alpha(1,2)\text{-S-S-}\alpha(3,4)]_2$, or “nicked protein”, likely to be structurally similar to the wild-type oxidized homodimer. A sigmoid-like shape for the transition curve thus resulted from the thermal unfolding of $\alpha(1,2)\text{-S-S-}\alpha(3,4)$, indicative of a cooperative process like those found in globular proteins.⁵³ Nevertheless, further experimental evidence was needed to conclude that the peptide was capable of self-assembly, as will be discussed later.

The promising preliminary results obtained with $\alpha(1,2)\text{-S-S-}\alpha(3,4)$ prompted us to explore via CD spectroscopy the structural behavior of $\alpha(1)\text{-S-S-}\alpha(4)$ and $\alpha(2,3)$ when mixed



Figure 6. Air oxidation of an equimolar mixture of $\alpha(1,2)$ -SH and $\alpha(3,4)$ -SH ($75 \mu\text{M}$ of peptide in 5 mM aqueous phosphate buffer, pH 7.1, 20°C , 4 h). HPLC conditions: linear gradient from 20% to 60% B; A, $\text{H}_2\text{O} + 0.045\%$ TFA and B, MeCN + 0.036% TFA; 1 mL/min, 220 nm. (a) $\alpha(1,2)$ -SH, (b) $\alpha(3,4)$ -SH, (c) $\alpha(1,2)\text{-S-S-}\alpha(3,4)$, (d) $\alpha(1,2)\text{-S-S-}\alpha(1,2)$, and (e) $\alpha(3,4)\text{-S-S-}\alpha(3,4)$.

together to allow mutual interaction. In this case, if fragment complementation were to occur, four peptide units would be necessary for the noncovalent assembly of a complex that could be structurally comparable to the native UG molecule. As previously observed in our laboratory for $\alpha(1)\text{-S-S-}\alpha(4)$, $\alpha(2,3)$ has a disordered structure in water but tends to form an α -helix in the presence of TFE. Both peptides were mixed in water and left for several hours in order to promote interchain packing interactions between them. The mixture afforded a random coil-like CD spectrum highly resembling that corresponding to the sum of the CD spectra of the individual peptides, which had been recorded under identical conditions. A similar experiment was performed with the peptides in 30% aqueous TFE, but again, both spectra were practically indistinguishable. These results are probably due to the entropic cost of the heterotetrameric assembly of two structured molecules of each peptide from the highly flexible independent units.

Oxidation Studies. The lack of complementation between $\alpha(1)\text{-S-S-}\alpha(4)$ and $\alpha(2,3)$ shifted our focus to $\alpha(1,2)\text{-S-S-}\alpha(3,4)$; more insight on the structural properties that contribute to the stability of this peptide in water was sought. The absence of secondary structure in $\alpha(1,2)$ -SH and $\alpha(3,4)$ -SH suggested that the disulfide bridge could play a role in the mutual recognition of sequences 1–28 and 29–70 of the rabbit UG monomer. To explore this possibility, the behavior of an equimolar mixture of $\alpha(1,2)$ -SH and $\alpha(3,4)$ -SH was studied by HPLC, similarly to the case of $\alpha(1)\text{-S-S-}\alpha(4)$. As shown in Figure 6, the spontaneous oxidation of Cys residues in a few hours afforded the heterodimer $\alpha(1,2)\text{-S-S-}\alpha(3,4)$ as the main product ($75 \mu\text{M}$ concentration of each peptide, phosphate buffer at pH 7.1, room temperature). Lower peptide concentrations appreciably prolonged reaction times, but the same result was ultimately achieved. This behavior was also observed when scrambling was induced with the redox system cysteine/cystine

(53) Pace, C. N. *Crit. Rev. Biochem.* **1975**, *3*, 1–43.

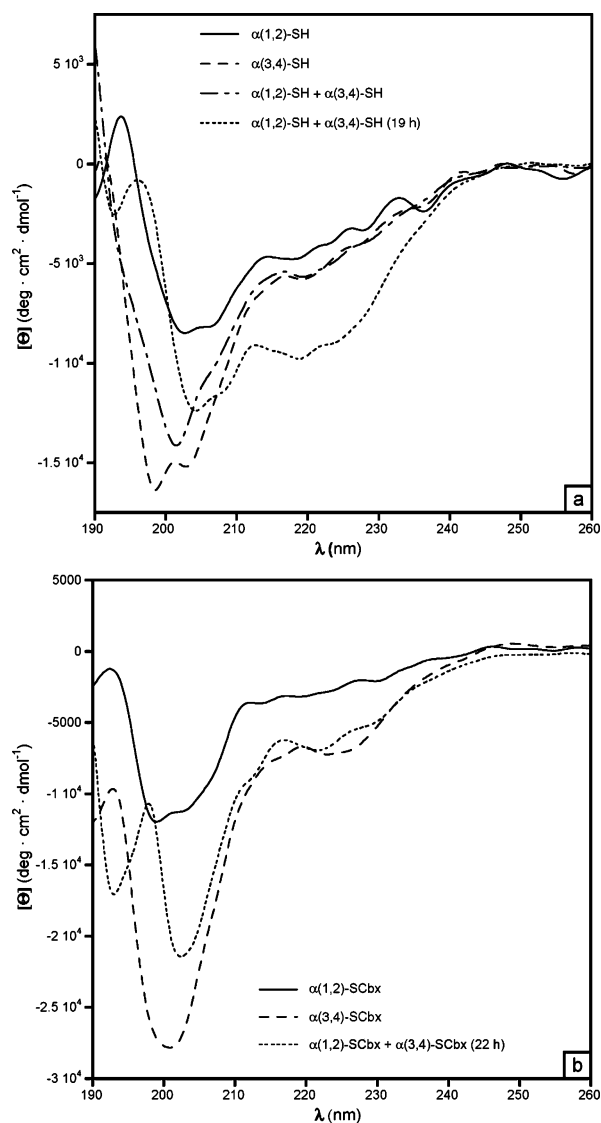


Figure 7. Far-UV CD spectra of individual and an equimolar mixture of (a) $\alpha(1,2)$ -SH and $\alpha(3,4)$ -SH; (b) $\alpha(1,2)$ -SCbx and $\alpha(3,4)$ -SCbx. Spectra were recorded at 25 °C in 5 mM phosphate buffer (pH 7.1) at 25 μ M concentration of each compound.

in a mixture of the homodimers $\alpha(1,2)$ -S-S- $\alpha(1,2)$ and $\alpha(3,4)$ -S-S- $\alpha(3,4)$.

These results could be explained in terms of interchain α -helix recognition as the driving force for selective heterodisulfide formation. This assumption would be in agreement with the fact that the homodimers do not express helicity in water and have helical propensities even lower than those of the corresponding monomers. Interestingly, the mixture of $\alpha(1,2)$ -SH and $\alpha(3,4)$ -SH did not initially give rise to any secondary structure, as revealed by CD. However, helicity slowly appeared with concomitant covalent heterodimer formation (Figure 7a). The lack of structure in the absence of the disulfide bridge is in agreement with the fact that reduction of $\alpha(1,2)$ -S-S- $\alpha(3,4)$ with dithiothreitol (DTT) yielded the monomers with complete loss of helicity (Figure 5b). On the other hand, no helical structure was detected, even after a long period of time, when oxidation was circumvented by using the carboxymethylated peptides $\alpha(1,2)$ -SCbx and $\alpha(3,4)$ -SCbx (Figure 7b).

Unlike the loss of helicity observed upon reduction of $\alpha(1,2)$ -S-S- $\alpha(3,4)$ and S-carboxymethylation, the CD spectra for

oxidized and reduced recombinant rabbit UG were very similar (Figure 5b). The behavior observed for UG under reductive conditions is consistent with literature precedent^{18,54} and suggests a secondary role of disulfide bridges in the stabilization of the tertiary structure. However, a different conclusion has to be reached for the heterodimer if the aforementioned experimental evidence is taken into account. Thus, there is no doubt that the disulfide bridge native to the protein is necessary to promote structure in $\alpha(1,2)$ -S-S- $\alpha(3,4)$. Heterodimeric disulfide formation is thus most likely favored by incipient interactions between α -helical conformations at the N-terminal and C-terminal of peptide sequences 1–28 and 29–70, respectively, which appear in the earliest conformational events of folding and are stabilized by local interactions.⁵⁵ The intermediates formed in these initial stages of folding occur on the microsecond time scale, and as a consequence, they can only be studied using sufficiently fast detection techniques.⁵⁶ Once the disulfide bond has been formed, it could drive the folding of $\alpha(1,2)$ -S-S- $\alpha(3,4)$ by helping to stabilize secondary structure through interchain interactions. In other words, the disulfide bridge would overcome the entropic cost of restricting the peptide chains to allow stabilizing contacts between them.⁵⁷

Ultracentrifugation and Fluorescence Spectroscopy. The assumption that the peptide $\alpha(1,2)$ -S-S- $\alpha(3,4)$ has to form noncovalent homodimers as a requirement to achieve folding was based on the dimeric nature of rabbit UG. However, CD spectra cannot confirm this idea because they provide only general information about secondary structure. The ability of the aforementioned peptide to adopt dimeric structures was assessed by both ultracentrifugation at sedimentation equilibrium and fluorescence spectroscopy.

The measurement and analysis of sedimentation equilibrium provides one of the most powerful and widely applicable methods for the characterization of reversible associations of macromolecules in solution.⁵⁸ It is based on the equilibrium concentration distribution that is obtained under centrifugal force. The behavior of a given macromolecule in solution is reflected by an exponential concentration gradient, and the equations that describe this behavior for systems such as single, non-interacting, or interacting macromolecular species are well established.⁵⁹ Samples of $\alpha(1,2)$ -S-S- $\alpha(3,4)$ at 71, 126, and 197 μ M concentrations in water containing 50 mM Tris buffer (pH 7.4) at 4 °C were submitted to sedimentation equilibrium to determine the association state of the peptide. Equilibrium was achieved at 22 000 and 31 000 rpm, and the cells were scanned at 278 nm. A set of superimposed curves was obtained when the experimental data obtained from all samples were overlaid on the same plot, and such behavior is typical of a reversibly self-associating system. This characterization was confirmed using a nonlinear regression analysis of absorbance versus radius

- (54) Hard, T.; Barnes, H. J.; Larsson, C.; Gustafsson, J. A.; Lund, J. *Nat. Struct. Biol.* **1995**, *2*, 983–989. (b) Peter, W.; Dunkel, R.; Stouten, P. F.; Vriend, G.; Beato, M.; Suske, G. *Protein Eng.* **1992**, *5*, 351–359. (c) Beato, M.; Arnemann, J.; Voss, H. J. *J. Steroid Biochem.* **1977**, *8*, 725–730. (d) Beato, M.; Baier, R. *Biochim. Biophys. Acta* **1975**, *392*, 346–356.
- (55) Yon, J. M. *Cell. Mol. Life Sci.* **1997**, *53*, 557–567.
- (56) Roder, H.; Shastry, M. R. *Curr. Opin. Struct. Biol.* **1999**, *9*, 620–626.
- (57) Wedemeyer, W. J.; Welker, E.; Narayan, M.; Scheraga, H. A. *Biochemistry* **2000**, *39*, 4207–4216.
- (58) (a) Cole, J. L.; Hansen, J. C. *J. Biomol. Tech.* **1999**, *10*, 163–176. (b) Lebowitz, J.; Lewis, M. S.; Schuck, P. *Protein Sci.* **2002**, *11*, 2067–2079. (c) Rivas, G.; Stafford, W.; Minton, A. P. *Methods* **1999**, *19*, 194–212.
- (59) Laue, T. M.; Stafford, W. F., III. *Annu. Rev. Biophys. Biomol. Struct.* **1999**, *28*, 75–100.

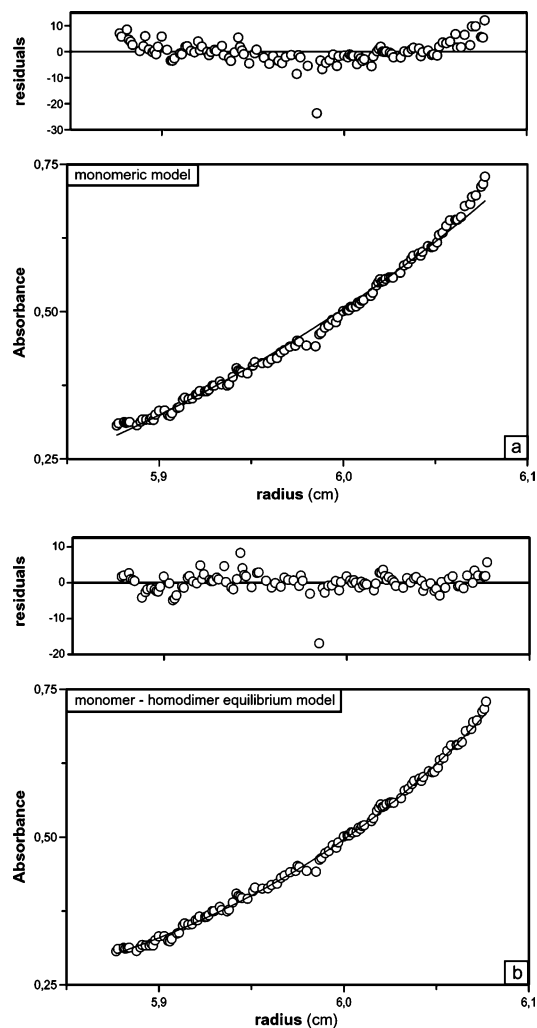


Figure 8. Sedimentation equilibrium analysis of $\alpha(1,2)$ -S-S- $\alpha(3,4)$. Solid lines shown in the lower panels are the result of fits to (a) a single ideal species and (b) a monomer–dimer equilibrium. Data points correspond to absorbance values at 278 nm. Upper panels show the difference in the fitted and experimental values as a function of radial position. The sedimentation equilibrium profile corresponds to a sample of $197 \mu\text{M}$ peptide in 50 mM Tris buffer (pH 7.4) at 4°C , and was taken at 22 Krpm.

data according to a monomer–dimer association model. As the random distribution of residuals shows (Figure 8), an excellent fit of the absorbance gradient was obtained when a monomer–dimer equilibrium model for a species with the molecular mass of $\alpha(1,2)$ -S-S- $\alpha(3,4)$ was considered (7958 Da). However, a deficient correlation resulted from the application of the model corresponding to an ideal non-interacting single component with the same molecular mass. The least-squares method used for the two species equilibrium model afforded a K_d value of $9 \pm 4 \mu\text{M}$, which confirms that the disulfide-containing heterodimer self-assembles noncovalently and with high affinity to form a tetramer.

Another way to assess the formation of this tetramer is to determine if small ligands are able to bind to the hydrophobic cavity formed upon interaction of two polypeptide chains. One of the goals of our research on UG structure is the exploration of the binding properties of its hydrophobic core. As mentioned above, a number of molecules have been shown to have a high affinity for UG, of which progesterone and 4,4'-bis[3-methylsulfonyl]-2,2',5,5'-tetrachlorobiphenyl] ((MeSO₂)₂TCB) have been the most studied owing to their potential physiological

implications. The numerous methods for studying substrate binding to UG can be divided into those using ¹H NMR techniques,⁶⁰ those based on spectrophotometric changes in the ligand upon binding,^{54c} and those employing radioactive ligands, the latter including equilibrium dialysis with microchambers,^{54d} gel exclusion techniques,⁶¹ and the charcoal-coated dextran procedure.^{19a} The fact that fluorescence has not been utilized to study UG can probably be attributed to the absence of tryptophan residues in the molecule as well as the low sensitivity of the tyrosine residues at positions 21 and 21'. Application of this technique to progesterone in our laboratory revealed minor changes in the fluorescence of tyrosine when steroid concentration was increased, and the K_d values obtained from these experiments were inconsistent with those reported in the literature (unpublished results). That prompted the use of a sensitive fluorescence probe with high propensity for binding to hydrophobic environments in order to reveal the dimeric nature of $\alpha(1,2)$ -S-S- $\alpha(3,4)$.

2-*p*-Toluidinylnaphthalene-6-sulfonate (TNS)⁶² has proven to be a convenient fluorescent probe for protein studies, as it weakly emits in water at about 500 nm but exhibits intense fluorescence at 425–460 nm upon binding to a hydrophobic matrix at the surface or in the core of a protein.⁶³ This property allows easy monitoring of bound TNS following the changes in emission intensity provoked by increasing amounts of probe. This spectroscopic behavior, along with the absence of absorption over 300 nm for UG and the molecular size and shape of TNS, moved us to choose this compound for carrying out a comparative study of its binding properties with the protein and the synthetic polypeptide. These experiments were performed using 7.5 and 15 μM concentrations of samples, respectively, in 10 mM phosphate buffer (pH 7.1) at room temperature. Rabbit UG and $\alpha(1,2)$ -S-S- $\alpha(3,4)$ were treated with increasing amounts of TNS, and the corresponding emission spectra resulting from excitation at 326 nm were recorded (Figure 9, insets). As reported earlier, the spectra were blue-shifted in both cases, the highest emission being raised at 423 and 429 nm, respectively, and the fluorescence intensities increased with increasing TNS concentration. Conversely, the probe did not fluoresce in the presence of a 1:1 mixture of $\alpha(1,2)$ -S-Cbx and $\alpha(3,4)$ -S-Cbx. These findings suggest that the complementary N-terminal and C-terminal chains spanning the monomer of rabbit UG are able to form a hydrophobic cavity when held together by the wild-type disulfide bridge, a conclusion that is in agreement with the random coil nature of the carboxymethylated peptides under these conditions, as observed by CD spectroscopy. The emission intensities obtained for rabbit UG and [$\alpha(1,2)$ -S-S- $\alpha(3,4)$]₂ at 422 nm were plotted against TNS concentrations, and the data were analyzed considering the formation of a 1:1 complex according to the results obtained for other UG-bound substrates (Figure 9).^{54a,64} A good fit was achieved in both cases, and the K_d values determined by the least-squares method used were

(60) Temussi, P. A.; Tancredi, T.; Puigdomenech, P.; Saavedra, A.; Beato, M. *Biochemistry* **1980**, *19*, 3287–3293.

(61) Fridlansky, F.; Milgrom, E. *Endocrinology* **1976**, *99*, 1244–1251.

(62) Weber, G.; Laurence, D. J. R. *Process Biochem.* **1954**, *56*, xxxi.

(63) (a) Brand, L.; Gohlke, J. R. *Annu. Rev. Biochem.* **1972**, *41*, 843–868. (b) Edelman, G. M.; McClure, W. O. *Acc. Chem. Res.* **1968**, *1*, 65–70. (c) McClure, W. O.; Edelman, G. M. *Biochemistry* **1966**, *5*, 1908–1919.

(64) Morize, I.; Surcouf, E.; Vaney, M. C.; Epelboin, Y.; Buehner, M.; Fridlansky, F.; Milgrom, E.; Mornon, J. P. *J. Mol. Biol.* **1987**, *194*, 725–739.

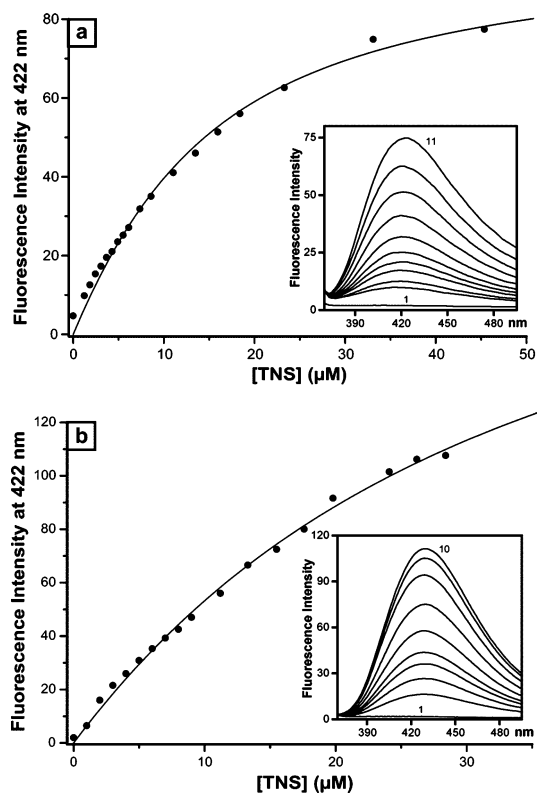


Figure 9. TNS titrations of (a) rabbit UG (7.5 μM) and (b) $\alpha(1,2)$ -S-S- $\alpha(3,4)$ (15 μM) in 10 mM aqueous phosphate buffer at pH 7.1. Emission intensity of TNS at 422 nm ($\lambda_{\text{excitation}} = 326$ nm) as a function of the concentration of the probe: (a) 0, 0.6, 1.2, 1.8, 2.5, 3.1, 3.7, 4.3, 4.9, 5.5, 6.1, 7.4, 8.6, 11, 13, 16, 18, 23, 33, and 45 μM ; (b) 0, 1, 2, 3, 4, 5, 6, 7, 8, 9, 11, 13, 16, 18, 20, 22, 24, 26, and 28 μM . Inset: Fluorescence emission spectra of the titration (a) [TNS] = 0 (spectrum 1) to 45 μM (spectrum 11), and (b) [TNS] = 0 (spectrum 1) to 28 μM (spectrum 10).

10.5 ± 1.1 μM for rabbit UG and 28.8 ± 2.8 μM for $\alpha(1,2)$ -S-S- $\alpha(3,4)$.

The UG analogues UG-[red] and UG-[Cbx] behaved with TNS analogously to the native protein, achieving maximum fluorescence intensity values at 426 nm in both cases. It is interesting to note that the affinities of the probe for these molecules were similar to that for native UG ($K_d = 7.9 \pm 0.9$ and 10.4 ± 1.3 μM , respectively), in contrast to what has been described for progesterone,^{54d} (MeSO₂)₂TCB,^{22c} and retinoids.²⁰ Thus, in these cases, the corresponding K_d values were up to 1 order of magnitude higher than those found for the native protein. According to the reports alluded to above, UG must be reduced in order for a substrate to suitably interact with the hydrophobic pocket. It is thus believed that the absence of disulfide bridges provokes conformational changes at the extremities of the monomers that allow a small molecule to access the cavity through the channel formed by helices $\alpha 1$ and $\alpha 4$ of both monomers.^{54b,65} However, recent docking experiments carried out with progesterone revealed that each monomer could independently rotate around the disulfide bonds to create an opening between the two monomers near the helix $\alpha 3$ region, creating an alternative route for the small molecule to slip into the hydrophobic cavity.⁶⁶ In this sense, our results could be explained in terms of the establishment of specific interactions

between TNS and this region of native UG that would favor entrance of the probe into the hydrophobic core of the protein.

Concerning peptide $\alpha(1,2)$ -S-S- $\alpha(3,4)$, the K_d values for TNS binding were 3–4 times higher than those found for the UG analogues. If it is assumed that the synthetic heterodimer forms a tetramer, its noncovalent nature compared to the disulfide-containing native molecule and a mutual recognition of the monomers less effective than in the case of UG-[red] and UG-[Cbx] could account for this result. Thus, whereas reduction and carboxymethylation of Cys residues in native UG do not lead to separation of the monomers,^{54c,67} cutting the chains between $\alpha 2$ and $\alpha 3$ probably increases the conformational flexibility of these helices, thereby reducing the stability of the resulting tetramer. On the other hand, the lower efficiency of the interchain hydrophobic contacts in the dimeric $\alpha(1,2)$ -S-S- $\alpha(3,4)$ may slightly modify the size and shape of the cavity, provoking changes in TNS fluorescence. An example of this phenomenon is N-substituted naphthylamine sulfonates, which are highly sensitive to the polarity of their immediate environments and whose maximum emission positions have been used to estimate values for binding site polarity.⁶⁸ From a qualitative point of view, the magnitude of the blue shift observed for the macromolecules studied in this work follows the order $\alpha(1,2)$ -S-S- $\alpha(3,4) < \text{UG-[red]} \approx \text{UG-[Cbx]} < \text{native UG}$, leading to the conclusion that TNS is surrounded by the less hydrophobic environment when bound to the synthetic peptide. However, the probe fluoresced under these conditions with a higher intensity than that induced by UG analogues (Figure 9), a result that could be explained in terms of the structural requirements of the excited state responsible for the emission band resulting from binding. Said state is thus believed to be a conventional $\pi \rightarrow \pi^*$ state that dominates in low-polarity environments and that is characterized by nonplanar orientation of the two aromatic rings in the probe.⁶⁹ Accordingly, the molecular rigidity of TNS when bound to UG may restrict the geometry suitable for optimal emission, whereas the probe would have enhanced flexibility into the hydrophobic pocket of the dimeric $\alpha(1,2)$ -S-S- $\alpha(3,4)$.

The native UG dimer has two symmetrically related internal Tyr residues that are involved in substrate binding.^{18,54a,70} It is believed that one or both of these residues interact with a small molecule that enters the cavity, helping to orientate the substrate to fit inside the hydrophobic core of the protein. Therefore, this residue is in close proximity to the steroid, a feature that could occur with other substrates. In the case of TNS, the spectroscopic properties of the molecule make fluorescence spectroscopy a suitable technique for obtaining specific information about such interaction in the protein and a hypothetical dimer of $\alpha(1,2)$ -S-S- $\alpha(3,4)$. As shown in Figure 10a, the emissions of rabbit UG and the covalent heterodimer due to Tyr residues have a large spectral overlap with the absorption of TNS. Dipole–dipole excitation transfer would therefore be possible, provided that the chromophore and fluorophore are within close proximity of each other, consequently providing an additional way to prove

(67) Nieto, A.; Ponstingl, H.; Beato, M. *Arch. Biochem. Biophys.* **1977**, *180*, 82–92.

(68) Turner, D. C.; Brand, L. *Biochemistry* **1968**, *7*, 3381–3390.

(69) (a) Karukstis, K. K.; Krekel, D. A.; Weinberger, D. A.; Bittker, R. A.; Naito, N. R.; Bloch, S. H. *J. Phys. Chem.* **1995**, *99*, 449–453. (b) Kosower, E. M. *Acc. Chem. Res.* **1982**, *15*, 259–266.

(70) (a) Dunkel, R.; Vriend, G.; Beato, M.; Suske, G. *Protein Eng.* **1995**, *8*, 71–79. (b) Peter, W.; Bruller, H. J.; Vriend, G.; Beato, M.; Suske, G. *J. Steroid Biochem. Mol. Biol.* **1991**, *38*, 27–33.

(65) Beato, M.; Saavedra, A.; Puigdomenech, P.; Tancredi, T.; Temussi, P. A. *Dev. Endocrinol.* **1980**, *8*, 105–119.

(66) Pattabiraman, N.; Matthews, J. H.; Ward, K. B.; Vaggi, G. M.-S.; Miele, L.; Mukherjee, A. B. *Ann. N.Y. Acad. Sci.* **2000**, *923*, 113–127.

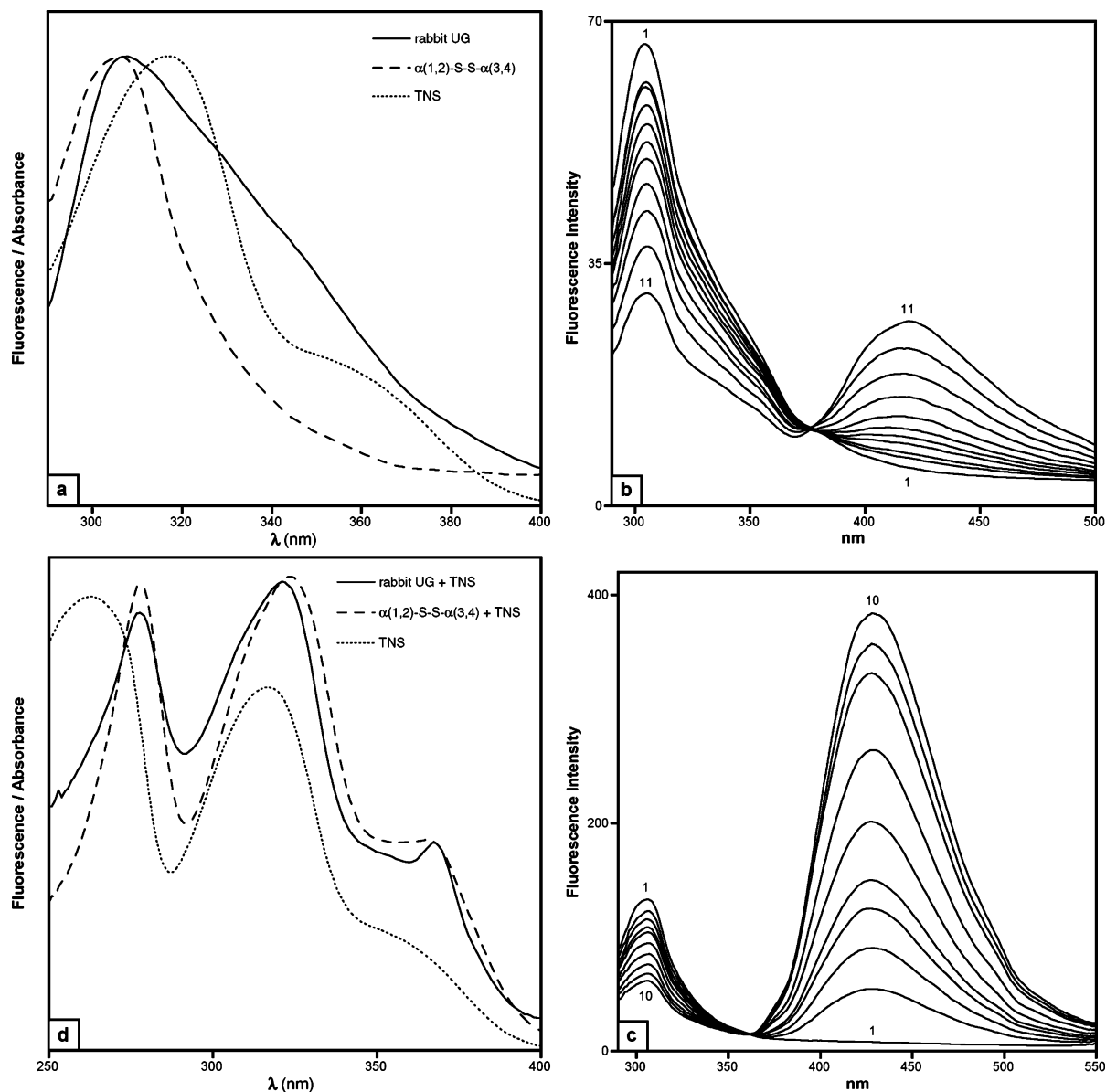


Figure 10. (a) Normalized fluorescence emission spectra ($\lambda_{\text{excitation}} = 279 \text{ nm}$) of rabbit UG ($7.5 \mu\text{M}$) and $\alpha(1,2)\text{-S-S-}\alpha(3,4)$ ($15 \mu\text{M}$), and absorption spectrum of TNS ($24 \mu\text{M}$). (b) Fluorescence emission spectra ($\lambda_{\text{excitation}} = 279 \text{ nm}$) of the titration of rabbit UG with TNS (same concentrations of TNS as reported in Figure 9). (c) Fluorescence emission spectra ($\lambda_{\text{excitation}} = 279 \text{ nm}$) of the titration of $\alpha(1,2)\text{-S-S-}\alpha(3,4)$ with TNS (same concentrations of TNS as reported in Figure 9). (d) Fluorescence excitation spectra ($\lambda_{\text{emission}} = 422 \text{ nm}$) of TNS in the presence of $7.5 \mu\text{M}$ rabbit UG ([TNS] = $8.6 \mu\text{M}$) and $15 \mu\text{M}$ $\alpha(1,2)\text{-S-S-}\alpha(3,4)$ ([TNS] = $6 \mu\text{M}$), and absorption spectrum of TNS ($24 \mu\text{M}$). Experimental conditions were similar to those described for Figure 9.

binding of the probe to the hydrophobic cavity.⁷¹ This feature was revealed when a fixed amount of rabbit UG or $\alpha(1,2)\text{-S-S-}\alpha(3,4)$ was titrated with increasing amounts of TNS, and the simultaneous changes in fluorescence emission with excitation at 279 nm of both polypeptide and polypeptide–TNS complex were monitored (Figure 10b,c). As shown in the figures, TNS molecules bound to the polypeptide efficiently quenched the Tyr fluorescence (λ_{em} around 305 nm), while the probe emission excited by the intermolecular Tyr energy transfer simultaneously appeared. As observed when excitation was carried out at 326 nm , the increase in TNS emission when forming a complex with $\alpha(1,2)\text{-S-S-}\alpha(3,4)$ was higher than that when bound to rabbit UG. Moreover, isoemissive points were observed at 377 nm for the native protein and at 362 nm in the case of the covalent heterodimer. These results confirm the presence of the

macromolecule in its free and TNS-bound states and that a Tyr residue at the least flanks the TNS binding site in both cases. An energy-transfer process was also confirmed when the excitation spectra of mixtures of rabbit UG or $\alpha(1,2)\text{-S-S-}\alpha(3,4)$ and TNS were recorded at 422 nm , which is the emission of TNS (Figure 10d). The spectra showed a band at 278 nm that does not appear in the absorption spectrum of TNS and corresponds to the absorption of Tyr, a result that demonstrates that the observed emission is specifically due to the amino acid.

Summary

Rabbit uterogloblin (UG) can be dissected into two identical homochiral halves either by the conventional reduction of the two disulfide bridges or via “la coupe du roi”. In the first case, which has been extensively studied in the literature and probably occurs in determined physiological conditions, two identical HS- $\alpha(1,2,3,4)\text{-SH}$ dithiol 70mers are formed. In the second case,

(71) Forster, T. *Ann. Phys.* **1948**, 2, 55–75.

reported for the first time in this paper, two identical homochiral halves are also formed (i.e., $\alpha(1,2)$ -S-S- $\alpha(3,4)$ disulfide 70mers). Independently of how UG is “dissected”, the two identical UG halves are able to form a globular noncovalent dimer, the folding of which is most likely driven by interhelical interactions. The importance and specificity of these interhelical interactions are highlighted by the ability of a mixture of $\alpha(1,2)$ -SH and $\alpha(3,4)$ -SH to regioselectively form $\alpha(1,2)$ -S-S- $\alpha(3,4)$ and, therefore, the noncovalent 140mer by spontaneous oxidation in aqueous solution. The results obtained in this work suggest that the “coupe du roi”-nicked UG could have interesting molecular recognition properties, suggesting its potential as a utile, readily synthesized framework for the design of biologically active molecules.

Experimental Section

Peptide Synthesis. Solid-phase peptide synthesis was carried out either manually in polypropylene syringes fitted with a polyethylene disk or automatically. Fmoc-amino acids were protected by the following groups: Boc for Lys; 2,2,5,7,8-pentamethylchroman-6-sulfonyl for Arg; *tert*-butyl for Asp, Glu, Ser, Thr, and Tyr; trityl for Cys, Asn, Gln, and His; and sulfoxide for Met. Boc-amino acids were protected by the following groups: *o*-chlorobenzoyloxycarbonyl for Lys; Tos for Arg; cyclohexyl for Glu; Bzl for Ser and Thr; *o*-bromobenzoyloxycarbonyl for Tyr; Npys for Cys; and benzyloxymethyl for His. Protected amino acids were purchased from Calbiochem-Novabiochem AG (Läufelfingen, Switzerland), Bachem Feinchemikalien AG (Bubendorf, Switzerland), Advanced ChemTech (Louisville, KY), or ProPeptide (Vert-le-Petit, France). Handles and the MBHA resin were obtained from Calbiochem-Novabiochem AG, and the PEG-PS resin was from Millipore Corp. (Bedford, MA). To swell the polymer, the resins were washed prior to the synthesis with dichloromethane (DCM) (4×1 min), 40% TFA in DCM (1×2 min and 1×15 min), DCM (4×1 min), 5% DIEA in DCM (4×3 min), DCM (4×1 min), and dimethylformamide (DMF) (4×1 min). Aminoacylations were monitored by qualitative ninhydrin⁷² or cloranil⁷³ assays and were repeated until negative test results were obtained. HF cleavages were performed in a standard HF reaction apparatus from Toho Kasei Co., Ltd. (Osaka, Japan).

Peptides were purified by RP-MPLC on a glass column containing Vydac C₁₈ (2.5×30 cm; $15\text{--}20 \mu\text{m}$, 300 Å). The equipment comprised a Duramat (CFG ProMinent) solvent delivery pump, an ABI 757 variable-wavelength absorbance detector, a Gilson FC 203 fraction collector, and an OmniScribe B-5000 chart recorder. A convex gradient at 125 mL/h was generated using two connected bottles (10×40 cm) containing different mixtures of MeCN/H₂O with 0.05% of TFA (400 mL each). Spectrophotometric monitoring was carried out at 220 nm, and fractions were collected every 3 min and analyzed by RP-HPLC. The fractions containing a single peak were collected and lyophilized. RP-HPLC was performed using a Vydac C₁₈ column (0.4×25 cm; $10 \mu\text{m}$, 120 Å) on a Shimadzu instrument consisting of two LC-6A solvent pumps, an SIL-9A auto injector, an SCL-6B system controller, an SPD-6A UV detector, and a C-R6A integrator. Linear gradients using mixtures of H₂O with 0.045% TFA (A) and MeCN with 0.036% TFA (B) were performed at 1 mL/min with detection at 220 nm (detection was also carried out at 340 nm in the case of $\alpha(1,2)$ -SNpys). Mass spectrometry (MS) was carried out on a Micromass VG-Quattro triple-quadrupole electrospray (ES) spectrometer (Manchester, UK) and on a PerSeptive Biosystems Voyager-DE time-of-flight matrix-assisted laser desorption–ionization (MALDI-TOF) spectrometer (Weiterstadt, Germany).

(72) Kaiser, E.; Colescott, R. L.; Bossinger, C. D.; Cook, P. I. *Anal. Biochem.* **1970**, *34*, 595–598.

(73) Christensen, T. *Acta Chem. Scand. B* **1979**, *B33*, 763–766.

$\alpha(1,2)$ -SH. The peptide was synthesized manually, starting from 1 g of PEG-PS resin with a loading value of 0.2 mmol/g. Prior to peptide chain assembly, the modified Rink amide linker (3 equiv) was coupled to the resin using DIPCDI (3 equiv) and HOBt (3 equiv) in DMF overnight. Amino acids (4 equiv) were anchored to the functionalized polymeric support with DIPCDI (4 equiv) in DMF (1 h) after Fmoc removal with 20% piperidine in DMF (2×1 min and 2×10 min). A single coupling protocol was used, although some exceptions were made. Thus, HOBt (4 equiv) was utilized for Asn, Arg, and Gln, and double couplings with DIPCDI and HATU (4 equiv)/DIEA (8 equiv) were performed for Thr.¹⁷ Upon completion of chain assembly, the Fmoc group of the N-terminal residue was removed, and the resin was washed with MeOH (3×1 min) and dried under vacuum (1.7 g) to obtain 1.7 g of peptidyl resin (f: 0.1 mmol/g). Full deprotection and cleavage of the peptide from the resin was accomplished by treating the resin (500 mg) with 4.5 mL of TFA containing H₂O (0.25 mL) and triethylsilane (0.25 mL) for 4 h at room temperature. The resin was separated by filtration, and the crude peptide was precipitated from the solution with Et₂O (10 mL) previously cooled to -78 °C. The supernatant was poured off after centrifugation, and the precipitate was washed with Et₂O (4×10 mL). The resulting material was dissolved in 10% aqueous AcOH, filtered, and lyophilized to obtain 123 mg of crude peptide. The product was purified in 40 mg batches using a gradient of 30–35% MeCN to yield 42 mg of peptide (13.5 μmol , 25%). ES MS (*m/z*): 3122.1 (MH⁺), C₁₄₂H₂₂₃N₃₆O₄₁S requires 3121.5.

$\alpha(3,4)$ -SH. The peptide was synthesized on a PEG-PS resin (0.2 mmol/g) to which the handle and the first amino acid were manually anchored before proceeding with automated chain assembly using a continuous-flow Millipore 9050 Plus synthesizer equipped with online UV monitoring. Thus, 3-(4-hydroxymethyl)phenoxypropionic acid (1.5 equiv) was coupled to the handle using DIPCDI (1.5 equiv) in DMF at room temperature overnight. After the resin was washed with DMF (4×1 min), it was loaded with Fmoc-Met(O)-OH (4 equiv) using DIPCDI (4 equiv) and DMAP (0.4 equiv) in a minimal amount of DMF. The mixture was allowed to stand for 1 h at room temperature, and a second coupling was performed. Further capping of the remaining hydroxyl groups was carried out by treatment of the resin with Ac₂O (10 equiv) and DMAP (1 equiv) in DCM for 20 min. The resin was then washed with DCM (4×1 min) and DMF (4×1 min), and the Fmoc group was cleaved to determine the resin loading.⁷⁴ Terminal amino deprotection was achieved with four treatments of 20% piperidine in DMF, two for 1 min and two for 10 min. The resin functionality was calculated from the UV absorbance (300 nm, $\epsilon = 7800$) of the released fulvene–piperidine adduct (0.19 mmol/g).

Amino acids (4 equiv) were preactivated with TBTU (4 equiv)/DIEA (4 equiv) in DMF for 5 min under bubbling N₂ and were coupled using the following protocol with a flow rate of 3 mL/min: DMF (15 s), 20% piperidine in DMF (1 min + 5 min), DMF (7 min), Fmoc-amino acid (5 s + 60 min), and DMF (4 min). Upon completion of chain assembly, the peptidyl resin was transferred to a polypropylene syringe fitted with a polyethylene disk, and the N-terminal Fmoc group was removed as described for the spectrophotometric determination of the functionalization. After the resin was washed with DMF (3×1 min), the amino groups were acetylated with Ac₂O (10 equiv) and DIEA (10 equiv) in DMF for 20 min. The resin was then washed with DMF (4×1 min) and MeOH (4×1 min) and vacuum-dried to afford 2.1 g of peptidyl resin (0.08 mmol/g).

A batch of 400 mg of resin was treated with a mixture of HF/Me₂S/*p*-cresol/*p*-thiocresol (1.25 mL:3.5 mL:0.25 mL:0.25 mL) for 4 h at 0 °C. Volatiles were removed under vacuum, and 4.5 mL of HF was added. The mixture was left for 1 h at 0 °C, and HF was removed under vacuum. The resulting material was washed with Et₂O, the crude peptide was dissolved in 10% aqueous AcOH, and the solution was lyophilized. The solid obtained was washed with Et₂O (4×10 mL),

(74) Ma, Y.; Sonveaux, E. *Biopolymers* **1989**, *28*, 965–973.

which was removed after centrifugation, and was dissolved again in 10% aqueous AcOH. The solution was filtered and lyophilized to afford 72 mg of crude peptide, which was purified by reverse-phase MPLC using a gradient of 25–40% MeCN to obtain 16 mg of the desired product (3.3 μmol , 15%). ES MS (m/z): 4838.8 (MH^+), $\text{C}_{205}\text{H}_{352}\text{N}_{54}\text{O}_{67}\text{S}_6$ requires 4837.4.

α -(2,3). The peptide was manually synthesized on a PEG-PS resin (500 mg, f: 0.31 mmol/g) to which the modified Rink amide linker was anchored. A single coupling with 4 equiv of handle and 4 equiv of DIPCDI overnight, and a double coupling using 1 equiv of the same reagents for 90 min at room temperature, were required in this case.

A single coupling of 1 h with DIPCDI (5 equiv) and HOBt (5 equiv) in DMF was used for aminoacylations, but additional couplings following different protocols were needed in some cases. Thus, Lys42 and Gln40 were attached using a double coupling protocol under the conditions mentioned above; Ala37, Thr33, Phe28 to Pro30, Pro18 to Ser24, and Gly16 were anchored with an additional coupling of 40 min with TBTU (3 equiv)/DIEA (6 equiv); and Leu25 and Thr17 required double coupling using this activating system. Removal of the Fmoc group was carried out as described for the synthesis of α -(1,2)-SH, and the protocol followed for the final amino acetylation and workup was that used for α -(3,4)-SH, yielding 1.3 g of peptidyl resin (0.11 mmol/g).

A batch of 100 mg of resin was treated with 1.2 mL of a mixture of TFA/anisole/thioanisole/ethanedithiol (90:2:3:5) at room temperature for 3.5 h, followed by addition of 20 μL of EDT (240 μmol) and 15.6 μL of trimethylsilyl bromide (120 μmol). The resulting suspension was left for 40 min at room temperature, at which point the crude peptide was precipitated with 12 mL of *tert*-butyl methyl ether (MTBE) at 0 °C. The supernatant was poured off after centrifugation, and the solid was washed with MTBE (3 \times 12 mL) and dissolved with 10% aqueous AcOH. Lyophilization (59 mg of crude peptide recovered) and purification by RP-MPLC using gradients of 25–40% MeCN (two batches) and 25–35% MeCN (two batches) afforded a total amount of 22.1 mg of pure peptide (5.9 μmol , 13%). MALDI-TOF MS (m/z): 3722 (MH^+), $\text{C}_{159}\text{H}_{255}\text{N}_{39}\text{O}_{57}\text{S}_3$ requires 3721.2.

α -(1,2)-S-S- α -(1,2). A 2 mM solution of α -(1,2)-SH (3 mL, 16 μmol) in 50 mM Tris buffer (pH 8) was left at room temperature under O_2 atmosphere for 24 h with vigorous magnetic stirring. The solution was lyophilized, and the resulting crude peptide was purified by RP-MPLC using a gradient of 35–40% MeCN to obtain 10.8 mg of homodimer (1.7 μmol , 60%). ES MS (m/z): 6242.2 (MH^+), $\text{C}_{284}\text{H}_{444}\text{N}_{72}\text{O}_{82}\text{S}_2$ requires 6241.

α -(3,4)-S-S- α -(3,4). A batch of 400 mg of the peptidyl resin obtained for the synthesis of α -(3,4)-SH was treated with 4 mL of a mixture of TFA/anisole/thioanisole/ethanedithiol (90:2:3:5) at room temperature for 4 h. To the filtered acidic solution was added Et_2O (10 mL), the resulting suspension was centrifuged, and the supernatant was removed. The solid thus obtained was washed with Et_2O (3 \times 10 mL) and dissolved in 10% aqueous AcOH. The solution was filtered and lyophilized to obtain 66 mg of crude peptide, which was purified by RP-MPLC using a gradient of 25–30% MeCN, yielding 41.7 mg of Met-protected peptide (8.5 μmol , 25%).

The peptide thus obtained (24.5 mg) was dissolved in 2.5 mL of TFA, and to the resulting solution (2 mM) were added 20 equiv of NH_4I and 20 equiv of Me_2S at 0 °C. The suspension was left for 6 h at 0 °C, after which 10 mL of H_2O and 25 mL of CCl_4 were added. The organic layer was removed, and the aqueous layer was washed twice with 25 mL of CCl_4 . Volatiles were removed under vacuum, and the resulting solid material was dissolved in 10% aqueous AcOH and lyophilized to afford 9.6 g of crude peptide. Purification by RP-MPLC using a gradient of 35–50% MeCN yielded 17 mg of the desired homodimer (1 μmol , 40%). ES MS (m/z): 9675.9 (MH^+), $\text{C}_{410}\text{H}_{712}\text{N}_{108}\text{O}_{134}\text{S}_{12}$ requires 9673.4.

α -(1,2)-S-S- α -(3,4). The synthesis of α -(1,2)-SNpys was performed on a MBHA resin following the Boc strategy. The peptide chains were

assembled on an ABI 430A automated peptide synthesizer, except for the amino-terminal sequence Gly-Ile-Cys, which was grown manually. Boc-amino acids were incorporated as symmetrical anhydrides or HOBt-activated esters in the case of the residues Asn and Arg, which were performed in an “activation vessel” before being transferred to the “reaction vessel” containing the starting resin (0.9 g, 0.56 mmol/g). Symmetrical anhydrides were prepared by adding 2 mL of a 0.5 M solution of DCC in DCM to the Boc-amino acid (4 equiv), which had been previously dissolved in 3 mL of DCM (a 10% of DMF was used in the case of Boc-Leu-OH), and leaving the mixture for 8 min. HOBt active esters were generated by dissolving Boc-amino acid in 4 mL of a 0.5 M solution of HOBt in DMF, to which 7–27% of DCM was added. The mixture was left for 6.5–8 min, at which point 2 mL of a 0.5 M solution of DCC in DCM was added and the residue was allowed to react for 33 min. Both activations were performed under bubbling N_2 . All activated amino acids were coupled once in 26–50 min with the exception of Asn, Arg, and the amino acids belonging to the sequence Gly1 to Leu13, which were coupled twice. Two additional couplings with HATU (4 equiv)/DIEA (12 equiv) were required to anchor Thr18. The α -amino protecting group was cleaved by treatment of the resin with 30% TFA in DCM for 80 s and 50% TFA in DCM for 18.5 min, followed by two 1 min treatments of 10% DIEA in DMF for neutralization. Upon completion of the peptide chain, the resin was washed with MeOH (3 \times 1 min) and vacuum-dried to obtain 1.2 g of peptidyl resin (0.09 mmol/g).

A batch of 500 mg of the peptidyl resin was treated with 4.5 mL of HF and 0.5 mL of anisole for 1 h at 0 °C. The resulting mixture was worked up as described for α -(3,4)-SH, which yielded 131 mg of crude peptide. Purification of the peptide by RP-MPLC using a gradient of 30–45% MeCN afforded 85 mg of pure product (49 μmol , 40%) as a pale yellow solid. ES MS (m/z): 3276.2 (MH^+), $\text{C}_{147}\text{H}_{224}\text{N}_{38}\text{O}_{43}\text{S}_2$ requires 3275.7.

To a 1 mM solution of α -(1,2)-SNpys (5 mL, 5 μmol) in 0.1 M aqueous AcOH (pH 4) was added α -(3,4)-SH (2.5 μmol , 0.5 equiv), and the resulting solution was stirred for 6 h at room temperature. The crude peptide recovered after lyophilization was purified by RP-MPLC using a gradient of 30–45% MeCN, which yielded 6 mg of heterodimer (0.75 μmol , 30%). ES MS (m/z): 7958.4 (MH^+), $\text{C}_{347}\text{H}_{572}\text{N}_{90}\text{O}_{108}\text{S}_7$ requires 7957.3.

Recombinant Rabbit UG. (i) Expression. Expression of rabbit UG was carried out in the Department of Molecular Genetics of the Molecular Biology Institute (Barcelona). Recombinant rabbit UG was expressed in *Escherichia coli* cells using the plasmid pT7 bearing the coding sequence of the protein. This cloning vector was kindly provided by G. Suske (Institut für Molekularbiologie und Tumorforschung, Phillips-Universität, Marburg, Germany). The plasmid (100 ng/ μL) was transformed into an *E. coli* strain BL21 (DES) by adding 2 μL of ADN solution to 100 μL of the cellular suspension and leaving the mixture for 2 min at 42 °C. The cells were then suspended in Luria-Bertani (LB) medium containing agar (1.5%) and ampicillin and incubated overnight at 37 °C to grow colonies. LB medium (5 mL) supplemented with ampicillin (50 $\mu\text{g}/\text{mL}$) was inoculated with a single culture and incubated for 5 h at 37 °C. An aliquot of 5 mL of the culture was diluted to 1 L with LB broth containing ampicillin (50 $\mu\text{g}/\text{mL}$) (OD_{600} of 0.1) and incubated at 37 °C to an OD_{600} of 0.7, at which point the expression was induced by adding isopropyl β -D-thiogalactopyranoside to a final concentration of 0.5 mM. After 2 h at 37 °C, the bacteria were harvested by centrifugation (15 min, 4000 rpm) and stored at -80 °C. Frozen bacteria were resuspended in 40 mL of aqueous 100 mM Tris/HCl buffer (pH 7.5) containing 150 mM NaCl and 5 mM DTT and lysed by sonication using six pulses of 30 s each at 1 min intervals. The resulting mixture was centrifuged (40 000 rpm), filtered through a 0.45 μm membrane, and stored at -20 °C.

(ii) Purification. The protein solution was chromatographed on a preparative Superdex-75 XK-16/100 column supplied by Pharmacia (100 \times 1.6 cm, 34 μm particle size), which was pre-equilibrated with

the solution buffer for 6 h. Samples of 0.5–1 mL were eluted at 1 mL/min with detection at 204 nm, and fractions of 10 mL were collected and analyzed on 18% sodium dodecyl sulfate–polyacrylamide gels. UG-containing fractions were pooled and dialyzed against 100 mM NH₄Ac (pH 8.0) using 1-cm-diameter Spectra/Por - 6 membranes (molecular weight cut off: 1 kDa), and the resulting solution was lyophilized. The protein was finally eluted on a reverse-phase Nucleosil-C₈ Vydac column (25 × 1 cm, 10 μm diameter, 300 Å pore size), using a linear gradient ranging from 20% to 80% MeCN–0.1% TFA in 30 min (1 mL/min, 220 nm). The UG-containing fractions were collected manually and pooled, and the resulting solution was lyophilized and stored at –20 °C. Amino acid analysis of the product afforded 322 nmol of protein as a homogeneous material by HPLC (19.5 min, 20–80% B in 30 min under the conditions described in this paper for peptide analysis). The dimeric nature of rabbit UG was assessed by ES MS, which revealed that the monomer had been partially expressed with an additional Met residue at the N-terminal position (15 927.6, C₆₉₀H₁₁₃₄N₁₇₈O₂₁₄S₁₄ + Met requires 15 927; 16 059, C₆₉₀H₁₁₃₄N₁₇₈O₂₁₄S₁₄ + 2Met requires 16 058).

Carboxymethylation of Free Cysteine Residues. The peptide or protein was incubated for 2 h in a buffer solution containing 150 mM Tris/HCl of pH 8.2, 6 M guanidine hydrochloride, and 35 mM DTT at 37 °C. Iodoacetamide was then added to a final concentration of 70 mM, and the mixture was incubated for 25 min at room temperature followed by lyophilization. The resulting crude material was purified by RP-HPLC (Vydac C₁₈, 25 × 1 cm, 10 μm particle size; A, H₂O–0.1% TFA and B, MeCN–0.1% TFA; 3 mL/min, 220 nm), and the product was determined to be homogeneous by HPLC (Nucleosil C-18, 25 × 0.4 cm, 5 μm; A, H₂O, 0.045% TFA and B, MeCN, 0.036% TFA; 1 mL/min, 220 nm). Yields were determined by amino acid analysis.

α(1,2)-SCbx: A 600 μM solution of the peptide (500 μL) yielded 126 nmol of pure product (42%) after chromatographic purification (15–100% B over 40 min). HPLC: 16.3 min (10–100% B over 30 min). ES MS (*m/z*): 3181.0, C₁₄₄H₂₂₅N₃₇O₄₂S requires 3178.6.

α(3,4)-SCbx: A 571 μM solution of the peptide (350 μL) yielded 81 nmol of pure product (41%) after chromatographic purification (15–100% B in 40 min). ES MS (*m/z*): 4895.5, C₂₀₇H₃₅₅N₅₅O₆₈S₆ requires 4894.8.

UG-[Cbx]: A 240 μM solution of the peptide (300 μL) yielded 4 nmol of pure product (5.6%) after chromatographic purification (15–80% B over 60 min). HPLC: 17.2 min (10–100% B over 30 min). MALDI-TOF (3,5-dimethoxy-4-hydroxycinnamic acid) (*m/z*): 8015.3, C₃₄₉H₅₇₇N₉₁O₁₀₉S₇ requires 8014.3.

UG-[red] and reduced α(1,2)-S-S-α(3,4) were obtained by treatment of the corresponding precursors in 5 mM aqueous sodium phosphate buffer (4.2 and 12.8 μM, respectively) with DTT (2 mM) for 2 h at 37 °C. The resulting solutions were used for spectroscopic studies without further purification.

Circular Dichroism Spectra. CD spectra were recorded from 260 to 190 nm using a Jasco J-720 spectropolarimeter with the sample compartment heated by a Neslab RP-100 circulating water bath. Samples were placed in square quartz cells with a path length of 0.1 cm, and measurements were made with a step size of 0.2 nm, a bandwidth of 1 nm, and an averaging time of 4 s. Spectra were averaged over two scans at a scan speed of 10 nm/min. CD data are reported in mean residue ellipticity (deg cm² dmol^{–1}):

$$[\Theta] = \frac{\Theta}{10cnl}$$

where Θ is the ellipticity in mdeg, *c* is the molar concentration, *n* is the number of residues of the protein or the peptide, and *l* is the path length of the cuvette in cm. The percentage *f* of peptide helical content was calculated by using the mean residue ellipticity at 222 nm and the

equation for the chain dependence of helices according to Yang et al.⁷⁵

$$f_{\%} = ([\Theta]/[\Theta]_{\alpha}) \times 100 \quad [\Theta]_{\alpha} = [\Theta]^{\infty}(1 - k/n)$$

where [Θ] is the observed mean residue ellipticity of the peptide, [Θ]_α is the mean residue ellipticity for the peptide in a 100% helical conformation, [Θ][∞] is the maximum mean residue ellipticity of a helix of infinite length (–39 500 at 222 nm), *n* is the number of amino acid residues, and *k* is a wavelength-dependent constant (2.57 at 222 nm).

Spectral analyses were carried out at 5 °C for individual samples or at 25 °C in binding experiments, and unspecified solvent dichroic ellipticity was subtracted from the spectra by software manipulation. The concentrations of UG analogues were 4.2 μM (wild-type and UG-[red]) and 12.8 μM (UG-[Cbx]), and those of the peptides were 20 μM (α(2,3), α(1)-S-S-α(4)) and 25 μM (α(1,2)-SH, α(1,2)-SCbx, α(3,4)-SH, α(3,4)-SCbx, α(1,2)-S-S-α(3,4)). Aqueous peptide and protein solutions used for the spectral analyses were prepared by taking aliquots from concentrated stock solutions in water (10–32 μM for UG analogues and 41–160 μM for peptides), lyophilizing, and dissolving the samples in freshly prepared 5 mM sodium phosphate buffer solution (pH 7.1) or TFE-containing buffer if required for titrations. For the spontaneous oxidation of α(1,2)-SH and α(3,4)-SH, the peptides were mixed in a 0.1 cm path length cuvette (25 μM of each), and spectra were recorded at time intervals whereby the acquisition time was less than 1% of the time required for completion of the reaction. A similar protocol was followed in the CD experiments performed with the mixtures α(1,2)-SCbx/α(3,4)-SCbx (25 μM of each) and α(2,3)/α(1)-S-S-α(4) (20 μM of each), which were compared with the corresponding theoretical sums of spectra of the isolated peptides calculated by using the equations [Θ]_{sum} = [Θ]_{α(1,2)-SCbx} × 28/70 + [Θ]_{α(3,4)-SCbx} × 42/70 and [Θ]_{sum} = [Θ]_{α(2,3)} × 33/70 + [Θ]_{α(1)-S-S-α(4)} × 37/70, respectively. Thermal denaturing of UG (5 μM) and α(1,2)-S-S-α(3,4) (20 μM) was followed by monitoring ellipticity at 222 nm from 10 to 90 °C automatically in 0.5 °C steps, with a data averaging time of 4 s and at a heating/cooling rate of 20 °C/h.

Ultraviolet Measurements. UV spectra were recorded on a Cary 500 spectrophotometer using 1 mL cells (0.1 cm optical path length) at room temperature. Solutions of UG and TNS in 10 mM sodium phosphate buffer (pH 7.1) were utilized in the experiments at concentrations of 7.5 and 24 μM as determined by amino acid analysis and gravimetry, respectively. Data were collected at a scan rate of 120 nm/min using a step size of 1 nm, with a 2 nm bandwidth and a 0.5 s averaging time. The absorbance was scanned from 250 to 500 nm, and all spectra were corrected for the background buffer contribution.

Fluorescence Spectra. Fluorescence measurements were made in 10 mM sodium phosphate buffer at pH 7.1, with an Aminco Bowman Series 2 fluorimeter equipped with a 150 W xenon lamp as the exciting source. Spectra were collected in 1 mL quartz cuvettes (0.1 cm optical path length) and maintained at 25 °C in a sample compartment heated by a Haake DC10 circulating water bath. The excitation wavelength for binding experiments was 326 nm, and emission was monitored from 370 to 590 nm. For the energy-transfer experiments, spectra were recorded with the excitation wavelength set at 278 nm, and emission was recorded from 290 and 540 nm. Detection was performed at 1 nm intervals in both cases, and data acquisition was carried out at a scan rate of 120 nm/min, with an excitation and emission band-pass set at 4 nm in all experiments. A 15-point smoothing algorithm was applied to the spectrum when a lower signal-to-noise ratio was obtained.

Determination of the Dissociation Constants. The binding affinities of TNS to UG, UG-[red], UG-[Cbx], and α(1,2)-S-S-α(3,4) were evaluated by analysis of the corresponding titration curves, monitoring TNS fluorescence as a reporter of the amount of complex containing TNS. The experiments were carried out using 7.5 μM solutions of UG

(75) Yang, J. T.; Wu, C. S.; Martinez, H. M. In *Methods Enzymol.* **1986**, *130*, 208–269.

and UG-[red], a 4.5 μM solution of UG-[Cbx], and a 15 μM solution of $\alpha(1,2)\text{-S-S-}\alpha(3,4)$ (450 μL in all cases). With the objective of covering the range of TNS concentrations studied (up to 40–46.3 μM), two concentrated standard solutions of the fluorescent probe were utilized (275 μM and 1.1 mM for the experiments with UG; 450 and 900 μM for the remaining assays). Thus, aliquots of 1 or 2 μL from these solutions were sequentially added to the solution of the macromolecule in the fluorescence cell, and the equilibrium fluorescence emission spectra were registered after 3 min of incubation of the mixtures with the prepared solution (10 mM phosphate buffer at pH 7.1, 25 $^{\circ}\text{C}$). The maximum change in volume was lower than 7% in all series of experiments. The fluorescence values of a blank buffer solution containing the added TNS were subtracted for each experiment, and correction of the emission spectra was made for variation in sensitivity of the photomultiplier with wavelength.

Assuming a 1:1 stoichiometry for the complex, the binding constant at equilibrium is defined by eq 1,

$$K_b = [\text{P:L}]/[\text{P}][\text{L}] \quad (1)$$

where [P], [L], and [P:L] are the concentrations of protein or peptide, TNS, and the complex, respectively. Considering in this case that neither the ligand alone nor the macromolecule fluoresces at the wavelength that was used for the determination of K_d (422 nm), the fraction of complex ($[\text{PL}]/[\text{P}_0]$) is expressed as

$$[\text{PL}]/[\text{P}_0] = F/F_S \quad (2)$$

where F_S is the fluorescence intensity at saturation, F is the observed fluorescence intensity, and P_0 is the total protein or peptide concentration ($[\text{P}] + [\text{P:L}]$). By rearranging eq 1 with eq 2, the observed F is given by

$$F = F_S \frac{([\text{P}_0] + [\text{L}_0] + K_d) - \sqrt{([\text{P}_0] + [\text{L}_0] + K_d)^2 - 4[\text{P}_0][\text{L}_0]}}{2[\text{P}_0]} \quad (3)$$

$[\text{L}_0]$ is the total concentration of TNS ($[\text{L}] + [\text{P:L}]$). The values of K_d and F_S were estimated from eq 3 by curve-fitting analysis of the plot of fluorescence intensity versus TNS concentration using the nonlinear least-squares procedure employing the ORIGIN data analysis program (Microcal Software Inc., Northampton, MA).⁷⁶

Analytical Ultracentrifugation. Analytical ultracentrifugation was performed in a Beckman Optima XL-A/I analytical ultracentrifuge equipped with a scanning absorption optical system at the Biochemistry Department of the UT Southwestern Medical Center at Dallas (Texas). Sedimentation was carried out at 4 $^{\circ}\text{C}$ in 50 mM Tris buffer solutions (pH 7.4) and was monitored at 278 nm. The number of radial points recorded was 1206 (step size of 0.001 cm), and five data points were collected and averaged at each radius. The experiments were run using a four-hole An-60 titanium rotor with three three-channel double-sector cells (1.2 cm optical path length) equipped with quartz windows and

a counterbalance. Two rotor speeds (22 000 and 32 000 rpm) and three samples of $\alpha(1,2)\text{-S-S-}\alpha(3,4)$ at different concentrations (71, 126, and 197 μM) were used in order to validate a reversible monomer–dimer association system. The time required to attain equilibrium was determined by running at a given rotor speed until the scans were invariant, using data acquisition times of 21 h at 22 000 rpm and 48 h at 32 000 rpm.

Equation 4⁵⁹ was used to analyze the sedimentation equilibrium data for $\alpha(1,2)\text{-S-S-}\alpha(3,4)$ as a reversible monomer–dimer association or as a single ideal species when $K_a = 0$:

$$c(r)_{\text{tot}} = c(o)_{\text{mon}} \exp[[M(1 - \bar{v}\rho)\omega^2/2RT](r^2 - r_o^2)] + K_a c(o)_{\text{dim}}^2 \exp[[2M(1 - \bar{v}\rho)\omega^2/2RT](r^2 - r_o^2)] \quad (4)$$

In this equation, $c(r)_{\text{tot}}$ and $c(o)$ are the total concentrations of the species in the solution (monomer and dimer) at a radial distance r and the concentrations of monomer or dimer at a reference radial distance r_o , respectively (mg/mL), M is the molecular weight (Da), ω is the angular velocity (rpm), \bar{v} is the partial specific volume of the molecule (L/g), ρ is the solution density (g/L), R is the gas constant, and T is the temperature (K). The analysis was performed using a partial specific volume of 0.73⁷⁷ for the covalent heterodimer ($M = 7958$ Da) and a density of 1.0 for the aqueous buffer solution.

Concentrations were plotted as absorbance values versus the radial distance, and the data were fitted to eq 4 using the nonlinear least-squares program ORIGIN. The resulting K_a values in A^{-1} units were converted to M^{-1} units via the following equation:⁷⁸

$$K_{\text{conc}} = K_a(\epsilon l)/2$$

where l is the optical path length (1.2 cm) and ϵ is the molar extinction coefficient of the peptide (2700 as the main value of those determined for the peptide samples used in the ultracentrifugation experiments). Samples of $\alpha(1,2)\text{-S-S-}\alpha(3,4)$ (110 μM) were prepared from a 411 μM peptide solution, as described for CD determinations.

Acknowledgment. This work was supported by funds from Ministerio de Educación y Cultura – FEDER (BIO2002-02-02301) and Generalitat de Catalunya (CeRBA and Grup Consolidat). We are very indebted to Dr. Dolors Ludevid of the Department of Molecular Genetics at the Molecular Biology Institute of Barcelona (Spain) and Dr. Josep Rizo of the Department of Biochemistry at the UT Southwestern Medical Center at Dallas (Texas) for providing free access to their laboratory facilities, for assistance in the expression of rabbit uteroglobulin and in the collection of ultracentrifugation data, respectively, and for fruitful discussions. We are also grateful to *Ministerio de Ciencia y tecnología* and *Generalitat de Catalunya* for support of this research through predoctoral fellowships.

JA0539793

(77) Tsai, J.; Taylor, R.; Chothia, C.; Gerstein, M. *J. Mol. Biol.* **1999**, *290*, 253–266.

(78) McRorie, D. K.; Voelker, P. J. *Self-Associating Systems in the Analytical Ultracentrifuge*; Publication 362784; Beckman Instruments, Inc.: Fullerton, CA, 1993.

(76) Johnson, M. L.; Correia, J. J.; Yphantis, D. A.; Halvorson, H. R. *Biophys. J.* **1981**, *36*, 575–588.